

## ABSTRACT

GUERTIN, EMMA, Developing a Robust Anaerobic Digestion Process for Co-Digestion of Food Waste and Municipal Solid Waste. (Under the direction of Dr. Francis de los Reyes).

Growing populations and energy demands require progress towards a circular economy where wastes are transformed into resources. About 30 to 40% of the US food supply is wasted (USDA), mostly ending up in municipal landfills. This food waste can be used as a substrate in anaerobic co-digestion (AcD) to increase biogas production from reactors and reduce greenhouse gas emissions from landfills. However, AcD of food waste requires process optimization. This project aims to identify mixtures of food wastes that result in optimum methane production and understand how microbial communities respond to shifts in mixtures of food waste types.

Initially, 21 reactors were loaded with various food wastes in a unique simplex centroid mixture design. Three reactors served as controls, and 18 were fed either cellulosic, proteinaceous, or fat-rich (lipid) waste. Once methane generation passed peak production, one reactor from each category was destructively sampled for microbial community analysis. The remaining reactors were fed a combination of 50% of their original food waste type and 50% of a new one. Again, once methane generation passed peak production, one reactor from each food waste combination was destructively sampled. The remaining reactors were fed an equal part mixture of the three food waste types. The protein-based reactors exhibited a large reduction in peak production after being introduced to either a lipid or carbohydrate substrate. Lipid-based reactors experienced a decrease in peak production rate but an increase in cumulative methane yield when introduced to carbohydrate waste. Carbohydrate-based reactors increased cumulative yield when introduced to either protein or lipid waste. These results highlight the importance of pre-existing communities in responding to shifts in waste type, suggesting that communities formed from the carbohydrate substrate are more resilient to waste changes than the microbial communities formed from the

other substrate types. The statistical analysis of the cumulative methane yields found the lipid and carbohydrate mixture to be the most optimal for methane production. Molecular microbial community analyses of reactor samples to observe the shift in communities attributable to substrate shifts are ongoing. This study provides insight into microbial adaptation to substrate changes and informs the development of operational procedures to optimize the AcD of food waste.

© Copyright 2022 by Emma Guertin

All Rights Reserved

Developing a Robust Anaerobic Digestion Process for Co-digestion of Food Waste  
and Municipal Solid Waste.

by  
Emma Guertin

A thesis submitted to the Graduate Faculty of  
North Carolina State University  
in partial fulfillment of the  
requirements for the degree of  
Master of Science

Environmental Engineering

Raleigh, North Carolina  
2022

APPROVED BY:

---

Dr. Francis L. de los Reyes III  
Committee Chair

---

Dr. Morton A. Barlaz

---

Dr. Douglas F. Call

## **DEDICATION**

To my parents, Jason Guertin and Stephanie Prentiss-Norcross, who have dedicated the last twenty-four years towards building a foundation of support and encouragement for their three children to provide the tools needed to achieve their goals.

To my grandmother, Bette Prentiss, who has watched firsthand the world make room for women in STEM careers.

To my late best friend, Brittany Murch, who had similar career aspirations. I share this degree with her and her family in the memory of Brittany's dreams of being an engineer.

## **BIOGRAPHY**

Emma Guertin was born in Gardner, Massachusetts, on June 22, 1998, to Jason Guertin and

Stephanie Norcross. She spent her childhood growing up in the small town of Hubbardston, MA.

After earning her bachelor's degree in Civil Engineering at the University of Massachusetts

Amherst, she joined North Carolina State University in August 2020 to pursue her master's

degree in Environmental Engineering under the supervision of Dr. Francis Lajara de los Reyes

III.

## ACKNOWLEDGMENTS

With deepest gratitude, I would like to first thank my advisor Dr. Francis de los Reyes for the opportunity to join his research group and for his consistently patient and flexible mentorship during the last two years. I am also thankful for Dr. Barlaz, Dr. de la Cruz, and Dr. Call for their expertise and guidance throughout this project.

I would like to extend my most sincere gratitude to fellow graduate students and friends Seraphim Falterman, Morgan DiCarlo, Savanna Smith, Leah Weaver, Hezhou Ding, and Yi-Chun Lai, who have offered their help at all different stages of this project from data collection to analysis. This thesis could not have been completed without their generous help.

I would also like to thank my parents, Jason and Stephanie, siblings Molly and Andy, and my great friends Victoria, Carina, Haley, Hayley, and many others for their unconditional support. Finally, I am thankful for all my graduate school friends that have provided many laughs and endless encouragement throughout this challenging journey.

## TABLE OF CONTENTS

LIST OF TABLES .....	vi
LIST OF FIGURES .....	vii
<b>Chapter 1: Introduction</b> .....	<b>1</b>
<b>Chapter 2: Review of Anaerobic Co-digestion of Food Waste Literature</b> .....	<b>5</b>
2.1 Introduction .....	5
2.2 Governing Processes and Parameters of Anaerobic Digestion .....	6
2.3 Known Benefits of Anaerobic Co-digestion .....	10
2.4 Food waste and Co-digestion Substrate Compositions .....	13
2.5 Microbiology of Food Waste Anaerobic Co-digestion .....	16
2.6 Future Work .....	18
<b>Chapter 3: Materials and Methods</b> .....	<b>19</b>
3.1 Experimental Design .....	19
3.2 Substrate and Inoculum Composition .....	23
3.3 Data Collection Methods .....	26
3.4 Data Analysis .....	28
<b>Chapter 4: Results and Discussion</b> .....	<b>29</b>
4.1 Loading Rate .....	29
4.2 Stage 1 Results and Discussion .....	31
4.3 Stage 2 Results and Discussion .....	38
4.4 Stage 3 Results and Discussion .....	45
4.5 Statistical Analysis Results and Discussion .....	50
<b>Chapter 5: Conclusion</b> .....	<b>58</b>

## LIST OF TABLES

Table 3.1	Sampling and loading schedule .....	20
Table 3.2	Composition of carbohydrate waste (wet weight %) based on US loss adjusted food availability data (USDA, 2017).....	25
Table 3.3	Composition of protein waste (wet weight %) based on US loss adjusted food Availability data (USDA, 2017).....	25
Table 4.1	Substrate COD concentrations .....	29
Table 4.2	Stage 1 Inoculum and Substrate Loading Rates .....	31
Table 4.3	Ammonia and COD concentrations beginning and end of Stage 1. The number in parenthesis on the ammonia concentrations represents the pH of the samples.....	36
Table 4.4	Stage 2 loaded food waste types and volumes .....	38
Table 4.5	Ammonia and COD concentrations beginning and end of Stage 2. The number in parenthesis on the ammonia concentrations represents the pH of the samples.....	43
Table 4.6	Stage 3 loading volumes.....	46
Table 4.7	Ammonia and COD concentrations beginning and end of Stage 3. The number in parenthesis on the ammonia concentrations represents the pH of the samples.....	49
Table 4.8	Results from the Scheffé linear model .....	52
Table 4.9	Scheffé Result from Quadratic Model.....	54
Table 4.10	Scheffé model results from special cubic model for stage 3 data .....	56

## LIST OF FIGURES

Figure 3.1	Unique Simplex centroid mixture design.....	20
Figure 3.2	Laboratory set-up at the beginning of Stage 1 of the experiment .....	22
Figure 3.3	Chopped fruit waste used for carbohydrate waste.....	23
Figure 3.4	Chopped vegetable waste used for carbohydrate waste .....	24
Figure 3.5	Cooked ground meat for the protein waste .....	24
Figure 4.1	Methane Production Rates for Stage 1 grouped as substrate types.....	32
Figure 4.2	Cumulative Methane yield during Stage 1 from all reactors grouped as substrate-based from loading in stage 1 .....	33
Figure 4.3	Averaged cumulative methane yields from replicate reactors in Stage 1 .....	34
Figure 4.4	Cumulative methane yields from Stage 1 from Carbohydrate-based reactors .....	34
Figure 4.5	Cumulative methane yields from Stage 1 from Lipid-based reactors .....	35
Figure 4.6	Cumulative methane yields from Stage 1 from Protein-based reactors .....	35
Figure 4.7	Methane production rates in Stage 2 .....	39
Figure 4.8	Cumulative Methane yield during Stage 2 from all reactors grouped as substrate-based from loading in stage 1 .....	40
Figure 4.9	Averaged cumulative methane yields from replicate reactors in Stage 2 .....	40
Figure 4.10	Cumulative methane yields from Stage 2 from Carbohydrate-based reactors .....	41
Figure 4.11	Cumulative methane yields from Stage 2 from Lipid-based reactors .....	41
Figure 4.12	Cumulative methane yields from Stage 2 from Protein-based reactors .....	42
Figure 4.13	Methane Production Rates for Stage 3 .....	46
Figure 4.14	Cumulative Methane yield during Stage 3 .....	47
Figure 4.15	Cumulative methane yields from Stage 3 from Carbohydrate-based reactors .....	47
Figure 4.16	Cumulative methane yields from Stage 3 from Lipid-based reactors .....	48

Figure 4.17 Cumulative methane yields from Stage 3 from Protein-based reactors .....	48
Figure 4.18 Contour Plot of Scheffé Linear Model Response Surface of Stage 1 Cumulative Methane Yield Data.....	51
Figure 4.19 Contour Plot of Scheffé Quadratic Model Response Surface of Stage 2 Cumulative Methane Yield Data.....	54
Figure 4.20 Contour Plot of Scheffé Special Cubic Model Response Surface.....	57

## CHAPTER 1: Introduction

Anaerobic co-digestion is an attractive tool for converting food waste to energy as populations and volumes of food waste continue to increase globally (Kaur et al., 2019). Utilizing food waste as a substrate in anaerobic co-digestion (AcD) would divert large sums of organic, putrescible waste from landfills. This could increase digester biogas production and serve as an alternative energy source. Lowering food waste volumes in landfills could also reduce the 14.5% of human-related methane emissions attributable to landfills (EPA, 2022). However, AcD of food waste requires process optimization for successful full-scale adaptation. Food waste composition is highly variable, and plant operators will not have much control over the source of food waste daily. Therefore, it is essential to understand how varying waste types will influence a digester system's performance.

To date, the impact of shifting food waste types on the microbial communities within an anaerobic digester is not understood. While there has been research on the chemical and microbial composition and the methane potential of food waste in AcD, the focus of previous work has been on singular waste types and not the influence of multiple waste types. This project addresses this knowledge gap by determining how various food waste types and mixtures impact methane production and microbial communities in lab-scale reactors. Understanding the impact of different food waste informs the development of operational procedures to optimize the performance of digesters and overcome perturbations due to shifts in substrate type.

A critical approach in addressing growing populations and energy demands coupled with implementing climate change mitigation practices is building a circular economy where waste products are transformed into resources. A significant waste category with potential for resource recovery is food waste. Food is wasted at all stages of the supply chain through agricultural

production, processing, distribution, and consumption (Papargyropoulou et al., 2014; Pramanik et al., 2019). The USDA estimates that 30 to 40% of food in the United States is wasted every year. In 2018, it was estimated that of the 63 million tons of food waste, 55% entered municipal landfills, representing the largest category of municipal waste (USDA, 2020). Another 12% of the food waste was incinerated. If not properly managed, these practices can have negative environmental impacts due to emissions of greenhouse gases, primarily methane (De Clercq et al., 2017; Levis & Barlaz, 2011). Landfilling food waste has additional environmental concerns, including odor and leachate production (Kaur et al., 2019). Developing strategies to divert food waste from landfills and incineration can significantly reduce our anthropogenic greenhouse gas emission rates (Nghiem et al., 2017; Papargyropoulou et al., 2014; Slorach et al., 2019). Anaerobic co-digestion can provide an alternative pathway for converting food waste to energy and close a gap in the circular economy.

Anaerobic digestion (AD) is a biological, sequential process that breaks down organic matter into biogas. This is accomplished through four stages, with process-specific microbes at each stage. The microbial community within anaerobic digestion systems is fundamental as the process requires a variety of microbes. In the first stage, hydrolysis, complex organic polymers such as carbohydrates, proteins, and lipids are broken down into soluble monomers such as sugars, amino acids, and long-chain fatty acids. This is typically the rate-limiting step in the anaerobic digestion of particulate wastes, such as biosolids or lignocellulosic materials. The monomers are converted into volatile fatty acids and alcohols through fermentative bacteria in the acidogenesis phase. Volatile fatty acids (VFAs) are often monitored during the AD process as the accumulation of VFAs can increase the system's acidity, which will inhibit methane production. Acetogenic bacteria then use VFAs to generate acetate, hydrogen, and carbon

dioxide. Methanogens utilize acetate, hydrogen, and carbon dioxide to produce methane and carbon dioxide in the last stage.

Mono-digestion of food waste, where food is the only substrate, has been found to have various process performance issues, such as low pH due to VFA accumulation, lack of metals and other necessary nutrients for microbes, and lack of a diverse microbial population to perform anaerobic digestion processes (Sillas-Moreno et al., 2019; Xu et al., 2014). Food waste co-digestion, the digestion of two substrates, has been found to improve digester performance by addressing some of these challenges (Karki et al., 2021; Lv et al., 2021a; Mehariya et al., 2018). Food waste is typically paired with municipal solid waste, animal manure, lignocellulosic waste, or biosolids to improve the system performance and increase biogas production (Lv et al., 2021a; Mehariya et al., 2018; Tyagi et al., 2018).

For full-scale plants, increasing biogas production is a profitable option. Biogas can be captured and utilized for a treatment plant to operate at energy neutrality, purified as a transport fuel, or injected into natural gas pipelines (Nghiem et al., 2017; Shen et al., 2015). Existing plants with anaerobic digestion reactors can use food waste to enhance their biogas production (Lv et al., 2021b; Pramanik et al., 2019). By operating at optimal conditions, plants can produce the maximum methane from their reactors and maximize profits. Understanding substrate composition is vital for optimal digestion performance as it influences the design loading rate, hydrolysis rate, available nutrients for microbes, and the microbial community within the system (Sanders et al., 2000; Speece, 1983; Wagner et al., 2013).

The high variability of food waste composition is a critical bottleneck in integrating co-digestion into full-scale treatment plants. There is a need to understand how the different compositions influence anaerobic digestion, specifically microbial communities and methane

production, to develop operational procedures. Past AcD research has focused on studying the influence of consistent substrate types with varying loading rates (Hagos et al., 2017; Karki et al., 2021; Lv et al., 2021a), but there is little understanding of how systems change and adapt when introduced to new substrate types. Specific microbial communities are attributable to different substrates (Wagner et al., 2013; Wang, 2018; Wei Zhang et al., 2014). Therefore, introducing a new substrate will require a resilient and robust microbial community to adapt. This knowledge gap needs to be filled to successfully utilize food waste as a co-digestion substrate.

This project aims to address this knowledge gap by studying the influence of various food waste types on methane production and the shift in microbial communities. First, mixtures of food waste that result in optimum methane production were identified by specifically using carbohydrate (fruits and vegetables), proteinaceous (meat waste), and lipid (fat-rich, such as fats, oils, and grease) waste. Second, how microbial communities respond to shifts in mixtures of food waste was assessed using microbial community analysis on samples taken throughout the experiment. These two objectives were investigated using lab-scale reactors loaded with various combinations of food waste mixtures to monitor process performance data and microbial communities. The results from this experiment can be used to develop operational procedures for full-scale adaptation, potentially allowing for digester control over methane yields and resilience to perturbations.

## CHAPTER 2: Review of Anaerobic Co-digestion of Food Waste Literature

### 2.1 Introduction

Resilient and robust anaerobic digestion processes for food waste need to be developed as global policies continue to restrict organic waste from landfills and waste volumes increase. The global population and generation of municipal solid waste continue to grow annually. By 2040, it is projected that food waste generated from households alone will increase to 220 million tons resulting in 180 metric tons of CO<sub>2</sub> emissions if current waste management methods persist (H. Zhang et al., 2020). In 2018, 63 million tons of food were wasted in the United States, the majority entering landfills or combustion facilities (EPA, 2020). Landfilling food waste has multiple associated environmental concerns, including greenhouse gas production, leachate toxicity, and odor production (Yunmin Chen et al., 2021; Levis & Barlaz, 2011). Globally, landfill restriction policies are starting to push toward environmentally beneficial food waste management practices. Sweden introduced a landfill ban in 2005 on organic waste, and Germany banned any un-pretreated organic waste from landfills (Dalke et al., 2021). These policies are starting to take hold in the United States, with state and local policies banning organic waste from landfills. California is the leading example, having banned organic waste from landfills and requiring organic waste collection services to be available to all residents and businesses (S. 1383, 2016). Vermont has a similar policy in place, requiring individuals to separate food residuals and arrange for the transfer of food residuals to a management option other than landfilling, such as digestion, composting, or land application (S. 6605, 2012). Washington and Massachusetts are not far behind with newer policies restricting companies and residents' ability to landfill food waste (Sandson & Broad Leid, 2021). As these policies continue to gain traction,

reliable food waste management options will need to be available to manage the waste stream diversion from landfills.

Anaerobic co-digestion (AcD) is an attractive alternative FW management method due to the associated environmental, technical, and economic advantages. AcD has been modeled as the most environmentally beneficial practice of food waste management options (Levis & Barlaz, 2011) due to the potential for biogas reuse. Food waste also can be introduced as a co-substrate to existing mono-digestion systems to increase biogas production, optimizing the economic benefits (Dalke et al., 2021; Nghiem et al., 2017).

## **2.2 Governing Processes and Parameters of Anaerobic Digestion**

Anaerobic digestion is a biochemical process of converting complex organic substrates into biogas. The process requires specific environmental conditions to achieve optimal performance, determined by the active microbial community within the system. Parameters to monitor and influence AD include pH, temperature, nutrient balance, intermediate products, and concentration of potential toxicants.

### *2.2.1 Governing Microbiology*

The active microbial communities in the digester govern anaerobic digestion. AD is a four-stage process, with process-specific microbes at each stage. A large and diverse microbial population is required to achieve a robust and resilient AD system. More microbial interactions may optimize resource utilization and increase methane production (Lin et al., 2016). The process begins with hydrolysis, where hydrolytic enzymes are produced and excreted by microbes to break down complex organics. The hydrolytic rate determines the overall waste stabilization and methane formation rate as it is often the rate-limiting step (Parkin & Owen, 1986). To ensure an efficient hydrolysis stage, a large and active population of hydrolytic

microbes needs to produce sufficient enzymes. Hydrolysis products are fermented into smaller acids or volatile fatty acids during acidogenesis (Parkin & Owen, 1986). These acids are then used to form hydrogen and acetate in acetogenesis. Hydrogen gas is also produced at this stage. Hydrogen concentration must be kept below partial pressure of  $\sim 10^4$  atm to avoid the accumulation of acids and subsequent inhibition of methanogenesis. Hydrogenotrophic methanogens can utilize hydrogen to produce methane, while acetoclastic methanogens use acetate to produce methane. In conventional AD processes, 72% of methane is formed from acetate cleavage, while the remaining 28% is created from  $H_2$  and  $CO_2$  (Parkin & Owen, 1986).

### *2.2.2 Temperature*

One of the most critical environmental conditions for AD is the operating temperature, as the temperature affects the metabolic activity of microbial communities, therefore impacting methane generation efficiency. Two ranges are traditionally recommended, mesophilic (35-40°C) and thermophilic (50-55°C). Thermophilic conditions have been found to enhance hydrolysis by improving hydrolytic activity. These conditions result in an increased rate and degree of organic matter destruction, improved dewatering conditions, and increased destruction of pathogenic bacteria (Parkin & Owen, 1986). Elevated temperatures can reduce the diversity of functional pathways but enhance the available pathways. This increases substrate conversion efficiency to methane but creates a less robust community due to less diversity. (Li et al., 2018; Lin et al., 2016). However, thermophilic methanogens are significantly less resilient than mesophilic methanogens as they are more sensitive to changes in temperature. Mesophilic conditions showed a higher resiliency and robustness due to a higher diversity of microorganisms but a less efficient substrate conversion compared to thermophilic. Additionally,

mesophilic digestion of FW has exhibited a capacity for higher organic loading rates due to the enhanced process stability and robustness (M. S. Kim et al., 2017).

### *2.2.3 pH*

The pH of an AD system is critical to continuously monitor as it often acts as a performance indicator of microbial community activity and gives insight into potential inhibitory effects. There are optimal pH ranges for each stage of the AD process. Methanogenesis is most influenced by pH as methanogens are sensitive to low pH. The system's pH typically drops at the beginning of the process due to volatile fatty acid (VFA) production and accumulation if hydrolysis and acidogenesis occur faster than the utilization of VFAs in acetogenesis and methanogenesis. Therefore, pH is often used to monitor the performance of the system. The alkalinity of the system mono-digesting food waste is usually required to balance pH from rapid hydrolysis. A pH range of 6.5 to 7.5 is generally accepted by literature as the optimal range for anaerobic digestion (Parkin & Owen, 1986; McCarty, 1964).

### *2.2.4 Micronutrients*

The concentration of various nutrients and metals is required for the optimal performance of microbes. Nitrogen and phosphorus are required in the highest concentrations. Nitrogen is used to synthesize proteins and enzymes in RNA and DNA. Phosphorus is necessary for bacterial growth and synthesis of energy storage compounds, RNA and DNA. To stabilize AD, trace metal concentrations are also needed in lower concentrations, such as nickel, iron, cobalt, sulfur, and calcium. Higher methane yields have been achieved from AcD of FW when appropriate levels of trace metals are available for process stability, allowing for higher organic loading rates. Trace elements can stabilize AD performance by reducing the lag phase,

increasing COD removal, and decreasing VFA build-up by stimulating methanogenic activity (Bardi & Aminirad, 2020; H. W. Kim et al., 2003).

The carbon to nitrogen ratio (C/N) is a crucial nutrient parameter to monitor within AD systems as there is an optimal ratio range for microbial activity. The C/N ratio greatly influences AD stability as it helps maintain a suitable environment for the microbial community (Pramanik et al., 2019). The optimal C/N ratio is widely accepted as 20 to 30 (Pramanik et al., 2019). A ratio too low indicates high ammonia concentration, leading to process instability. A too high ratio will mean not enough ammonia available for microbial growth and slow the degradation rates (Pramanik et al., 2019).

#### *2.2.5 Volatile Fatty Acids*

Volatile fatty acids (VFAs) are an intermediate product formed during acidogenesis. The accumulation of VFAs typically leads to acidic pH, resulting in the inhibition of methanogens. However, McCarty (1964) suggests that VFA concentrations of up to 6000 mg/L can be tolerated in a system with no loss of methane production if pH is maintained at the optimal range of 6.5 to 7.5. Propionic acid concentrations of 6000 mg/L are inhibitory to acetogenic bacteria. Unionized volatile acids, UVA, are toxic specifically to methanogens at much smaller concentrations (30 to 60 mg/L) (Parkin & Owen, 1986). Instead of using absolute VFAs, concentrations monitoring relative changes in VFAs in partnership with pH is more reflective of process stability (Li et al., 2018).

#### *2.2.6 Nitrogen Compounds*

Total ammonia nitrogen (TAN) is comprised of ammonium ion ( $\text{NH}_4^+$ ) and free ammonia ( $\text{NH}_3$ ). Ammonia is produced during the digestion of organics, especially from high protein substrates. High ammonia concentrations are inhibitory to the AD process, but a range of

ammonia concentrations is beneficial for buffering capacity. High ammonia levels will create a high pH that is not optimal for acidogenesis and cause a decrease in microbial activity (Rajagopal et al., 2013). There is a wide range in the literature defining beneficial and inhibitory concentrations. Beneficial concentrations of TAN range from 50 – 200 mg/L (McCarty, 1964). There is a wide range of inhibitory concentrations observed in AD. Concentrations above 1500 mg/L have reported a moderate inhibitory effect on methane production (Mehariya et al., 2018). A commonly accepted threshold of inhibition on methane production is 3000 mg/L for TAN at a pH greater than 7.4 (McCarty, 1964). However, multiple studies did not experience a reduction in methane generation until reaching much high TAN concentrations, ranging from 4000 to 10,000 mg/L, until experiencing inhibitory effects (Angelidaki & Ahring, 1994; González-Fernández & García-Encina, 2009). Free ammonia has shown to be more severely toxic at concentrations greater than 100 mg/L as it permeates cell membranes resulting in proton imbalance (Shi et al., 2017). Since pH significantly influences free ammonia concentration, neutralizing the system can alleviate ammonia toxicity and allow acclimation to higher concentrations.

## **2.3 Known Benefits of Anaerobic Co-digestion**

### *2.3.1 Technical Advantages*

Mono-digestion of food waste comes with many technical challenges. Due to the high biodegradability of FW, hydrolysis occurs rapidly, resulting in an accumulation of VFAs and subsequently creating an acidic pH in the system. Additionally, FW is low in critical metals and nutrients, specifically in metals needed for microbial activity. While it is high in carbon, it is low in nitrogen unless it is a protein-rich substrate, causing an imbalance in the critical C/N ratio—these challenges all impact methane generation and degradation efficiency in a system.

Adding at least one substrate to a digester with food waste can address these challenges by stabilizing the digester and supplementing additional essential microbes and nutrients needed for the AD process.

Accumulation of VFAS in AcD of FW results from rapid hydrolysis due to the high biodegradability of food waste and causes a subsequent drop in pH. Adding different feedstock to the system can increase the buffering capacity of the system to prevent this acidification. Buffering capacity can be increased by balancing the carbon/nitrogen (C/N) ratio within AcD using feedstock with abundant ammoniacal nitrogen. Animal manure has shown the ability to provide a strong buffer capacity to maintain a neutral pH despite a high concentration of VFA. Municipal solid waste leachate has also demonstrated strong buffer capacity against VFA acidification (Bi et al., 2020; Zhang et al., 2015a). Co-substrates can also provide trace elements that help degrade VFAs to avoid accumulation (Bardi & Aminirad, 2020; H. W. Kim et al., 2003). Various feedstock added to the monodigestion of food waste can supplement essential trace metals that food waste lacks. The lack of crucial TMs will inhibit methanogens' growth, impacting methane generation (Lv et al., 2021a). Adding feedstock with supplemental metals can promote microbial diversity, thus improving the system's robustness. MSW leachate and animal manure addition to FW digestion have been attributed to an increase in Fe, Co, Mo, and Ni concentration in the digestate, resulting in increased stability of the digester system (Zhang et al., 2015a). Additional trace elements such as Ca and Mg from co-feedstock can improve the digestate dewaterability (Lv et al., 2021a). Co-digestion has also resulted in a more diverse bacterial and archaeal population due to the supplement of microbes from the feedstock. Animal manure and biosolids have essential microbes for the AD process that can increase methane production from food waste by increasing microbial diversity, resulting in different available

methanogenetic pathways (Z. Wang et al., 2020). Microbial communities of food waste AcD are further discussed in section 2.5.

### *2.3.2 Environmental Advantages*

Based on life-cycle assessments of various management strategies, anaerobic digestion has been shown to be the most environmentally beneficial treatment option for food waste (Levis & Barlaz, 2011). This analysis included modeling anaerobic digestion, various aerobic composting systems, landfills with and without gas collection, and a bioreactor landfill to determine global warming potential, NO<sub>x</sub>, and SO<sub>2</sub> emissions. Anaerobic digestion proved the most environmentally beneficial treatment option, leading to -395 kg net CO<sub>2</sub> per 1000 kg of food waste. Diverting the waste from landfills to use for stabilizing digesters and increasing biogas production will significantly reduce greenhouse gas emissions from landfills (Nghiem et al., 2017).

### *2.3.3 Economic Advantages*

Anaerobic digestion practices exist in wastewater treatment plants, municipal waste treatment plants, and farms for manure management. Food waste can be utilized as a co-substrate at these existing plants to stabilize digesters and improve performance. This could increase digester biogas production. Increasing biogas production from these existing digesters could allow plants to operate at energy neutrality if they can capture the biogas and heat their plants. A dairy farm in New York combined food waste with their cattle manure that had been previously monodigesting. The addition of food waste increased their degree of waste stabilization during digestion (Dalke et al., 2021). A farm in Massachusetts implemented a digester to treat food waste and animal manure. The increase in co-digestion's biogas production allows them to offset 100% of their electricity costs (Dalke et al., 2021). Excess biogas can be sold to utilities or

injected into a pipeline beyond facility needs. The revenue from this will depend on local and state policies, regulations, and interconnectivity. Therefore, increasing biogas production increases profitability. Tipping fees also make FW AcD affordable, as the New York farm found AcD economically favorable from tipping fee collection alone.

## **2.4 Food waste and Co-digestion Substrate Compositions**

### *2.4.1 Municipal Solid Waste and Leachate*

Municipal solid waste (MSW) and MSW leachate have been shown as promising co-substrates for AcD with food waste. MSW is rich in trace metals and contains a high ammoniacal-nitrogen concentration that can stabilize digester performance and enhance biogas production in monodigestion of food waste. MSW can also provide microbes that can aid in the performance of AD. The ammoniacal nitrogen concentration in MSW leachate balances the C/N ratio in AD of FW, stabilizing anaerobic microbial activity and resulting in better digester performance than monodigestion (Shahbaz et al., 2019). The ammoniacal concentration also improves the buffering capacity of the system and avoids VFA inhibition from rapid hydrolysis of FW (Zhang et al., 2015b). Leachate addition can also increase methane production by supplementing trace metals that support the enzymatic activity of anaerobes (Lv et al., 2021a). MSW leachate has a diverse population of metals, such as Fe, Co, Mo, and Ni. Supplementing these metals by adding leachate has been found to increase the energy conversion rate of AcoD by 18% (Lv et al., 2021a). Stable methane yields from leachate addition to FW have ranged between 369 to 466 mL CH<sub>4</sub>/gVS (Liao et al., 2014; Lv et al., 2021a; Zhang et al., 2015b). Additionally, MSW leachate contains high concentrations of COD, contributing to biodegradable organics and methane potential. There is a balance required between leachate and food waste loading rates. Loading too high of a leachate volume to the system resulted in a lower C/N ratio

caused by the high ammonia nitrogen concentration and will create a basic pH (Liao et al., 2014; Shahbaz et al., 2019). Excess ammonia nitrogen is inhibitory to microbial activity and is related to free ammonia, the main factor affecting methanogenic microorganisms (Lv et al., 2021a). To avoid these challenges, Shabaz et al. (2019) found that the optimal mixture ratio of FW to leachate was 0.5, resulting in a C/N ratio of 20.

#### *2.4.2 Sewage Sludge*

A commonly used co-substrate with food waste is sewage sludge (SS) from wastewater treatment plants. The AD process was traditionally adopted for sewage sludge treatment and has been well studied in literature and widely adopted at full scale. AcD with food waste could be adopted at these existing plants and increase biogas production from existing facilities. SS has a high concentration of metals and a low C/N ratio. These characteristics pair well with FW, which has a low concentration of metals and typically a high C/N ratio. SS can supplement essential metals and provide buffering capacity to avoid VFA inhibition due to the low C/N ratio (Bardi & Aminirad, 2020; Mata-Alvarez et al., 2014; Mehariya et al., 2018). SS has a large population of active bacteria engaged in the AcD process. Supplementing microbial populations will enhance AD performance by increasing the system's diversity and, therefore, the robustness within the system. Additionally, FW can balance the C/N ratio of the SS and dilute heavy metals and pathogens that are often present. (Mata-Alvarez et al., 2014; Zheng et al., 2021).

This mutualistic relationship increases biogas production volume at optimal mixture ratios. Methane yields from different mixture ratios range from 157 to 439 mL CH<sub>4</sub>/g VS, which calculates an 18% to 97% increase in biogas production from monodigestion (Mehariya et al., 2018). Kim et al. (2003) achieved 214 CH<sub>4</sub>/g VS from a 50:50 mixing ratio on a volatile solid basis from lab-scale operated reactors in thermophilic conditions, showing an 85% biogas

production improvement compared to monodigestion. At full scale, the same ratio at mesophilic conditions produced 280 mL CH<sub>4</sub>/g VS, or a 97% increase from monodigestion of FW (Bolzonella et al., 2006). Bolzonella et al. (2006) found a two-fold increase in specific methane yield compared to monodigestion of SS.

### *2.4.3 Animal Manure*

Animal manure is another commonly used co-digestion substrate for AcD with food waste. Typically, cattle, swine, and poultry manure are the primary sources (Karki et al., 2021). Animal manure has a low C/N ratio, leading to process instability during mono-digestion caused by ammonia toxicity—adding carbon-rich FW addresses this issue by supplementing a higher C/N ratio to balance out the ammonia concentration (Karki et al., 2021). Zhang et al. (2013) found the optimal C/N ratio for AcD of cattle manure (CM) and FW to be 15.8. This was achieved through a mixing balance between FW/CM of 2 (based on VS). The high ammonia concentration in animal manure provides the same buffering capacity against VFA accumulation as found with SS and MSW and maintains a neutral pH. This buffer capacity allows for an increased organic loading without adding additional pH control (C. Zhang et al., 2013). Additionally, animal manure enhances trace metals and supplements relevant microbial populations, improving substrate degradation rates (Karki et al., 2021; C. Zhang et al., 2013).

Co-digestion of FW and animal manure result in increased biogas productions compared to the mono-digestion of either substrate due to the balanced C/N ratio, increased buffering capacity, and supplement of metals and relevant microbial communities. Biogas production increased by 41% during AcD of cattle manure and FW at a mixing ratio of 2 (VS basis) (C. Zhang et al., 2013). FW added to poultry manure increased specific methane yield by 93.4%, achieving 351 mL CH<sub>4</sub>/gVS added (Zahan et al., 2018).

## 2.5 Microbiology of Food Waste Anaerobic Co-digestion

Anaerobic co-digestion performance is reflective of the microbial community activity within the system. The microbial community is the most critical driver of anaerobic digestion. Most bacteria in AD belong to the phyla *Bacillota*, *Chloroflexota*, *Bacteroidota*, *Psuedomonadota*, and *Actinomycetota* (Karki et al., 2021). However, specific microbial communities and structures are attributable to different substrate types. Diverse microbial communities are required to utilize various substrate types (Wagner et al., 2013). For example, SS-fed AD systems have been found to have a high population of *Bacillota* and *Bacteroidota*, while manure fed systems have a higher population of *Chloroflexota* (Karki et al., 2021). Variations in food waste types have also resulted in different microbial structures. Different substrate types in a system can result in changes in the microbial community and provide insight into the system's resiliency towards utilizing various kinds of wastes.

Microbial populations during the AD of FW have been studied to determine the present and active bacteria and archaea during different stages of AD. Fermentative bacteria that are dominant during hydrolysis belong to *Bacillota* and *Bacteroidota*. These bacteria can decompose FW into soluble monomers and survive in various environmental conditions, proving more resilient than methanogens (Mehariya et al., 2018). *Clostridium* have been observed in protein, carbohydrate, and lipid conversion to monomers (Pramanik et al., 2019). Bacteria that convert proteins to soluble peptides and amino acids include *Proteus*, *Peptococcus*, *Vibrio*, *Bacteroides*, and *Bacillus* (Deepanraj et al., 2014). Carbohydrates are fermented to sugars by *Acetivibrio*, *Staphylococcus*, and *Bacteroides* (Deepanraj et al., 2014). *Micrococcus* and *Staphylococcus* are responsible for converting lipids to long-chain fatty acids (LCFAs) (Deepanraj et al., 2014). The monomers formed in hydrolysis are converted to simple molecules such as VFAs and CO<sub>2</sub>, and

H<sub>2</sub> by acidogenic bacteria. These bacteria belong to the phyla *Bacillota*, *Chloroflexota*, *Bacteroidota*, and *Pseudomonadota* (Mehariya et al., 2018). Sugars are converted to VFAs and alcohols mainly by *Clostridium*, while there is a diverse community that can convert amino acids, including *Lactobacillus*, *Escherichia*, and *Staphylococcus* (Deepanraj et al., 2014). Acidogenic bacteria utilize the VFAs and alcohols to produce acetate or H<sub>2</sub> and CO<sub>2</sub>. *Clostridium*, *Syntrophobacter*, and *Syntrophomonas* are responsible for this process. The final stage is methanogenesis, converting H<sub>2</sub>, CO<sub>2</sub>, and acetate into methane, accomplished by either acetoclastic or hydrogenotrophic methanogens. Acetoclastic methanogens utilize acetate for methanogenesis and belong to the *Methanosaeta* genus. Hydrogenotrophic methanogens use hydrogen gas to reduce CO<sub>2</sub> and mainly belong to the genera *Methanobacterium*, *Methanothermobacter*, *Methanobrevibacter*, *Methanospirillum*, and *Methanoculleus*. *Methanosarcina* can use H<sub>2</sub> and acetate to generate methane and is often viewed as the highest quality methanogen due to its high adaptability against environmental changes and tolerance of inhibitory substances (Zhang et al., 2021).

Changes in operational conditions such as loading rates and temperatures can easily influence the AD process. The influence manifests itself in the microbial community. Therefore, it is essential to understand the active and present microbial communities to develop a resilient and robust process to perturbances. Anaerobic co-digestion enhances the diversity of the bacteria and archaeal community due to the supplement of microbial communities, therefore creating a more robust system (Zhang et al., 2021). Microbial diversity is an essential measure of AcD efficiency. Added substrate results in synergistic effects, more available pathways for methane generation, and improved system resiliency. AcD of FW and various co-substrates have resulted in synergistic effects from the supplement of different relevant microbes. Co-digestion of FW

and CM showed synergistic effects of decreased VFA concentrations, significantly reduced lag phase, and faster peak methane production rate than the monodigestion of FW and CM (Zhang et al., 2021). AcD also provides various pathways for methane production by increasing the diversity of the archaeal community. The addition of CM to FW showed an enhanced archaeal community richness and diversity compared to monodigestion, indicating a vigorous methane production vitality in this studied system (Zhang et al., 2021). Zhang et al. (2021) observed that AcD of FW and CM sustained more diverse and switchable methanogenic pathways, ensuring powerful methanogenic functions and robust capability. The dominant methanogenic path was CO<sub>2</sub> reduction via hydrogenotrophic *Methanoculleus* (69%). In monodigestion of FW, the dominant genus of methanogen has been observed as *Methanosaeta*, indicating the influence of the substrate on methanogenic pathways (Li et al., 2015).

## **2.6 Future Work**

AcD of food waste needs to be continuously studied and optimized as the technology and waste collection logistics face challenges that have slowed full-scale adaptation. The influence of multiple food waste types on reactor performance has not been well documented. This is important as plants utilizing food waste as a co-substrate do not control the types of food waste they receive and need to understand how different compositions of food waste will impact digester performance. Specifically, this is understanding the relationship between the dynamic behavior of bacterial communities and food waste composition. Understanding how microbial communities react to changes in the composition will provide operational insight into different FW mixtures. This research project has focused on answering these knowledge gaps by monitoring the influence of different food waste types on methane production and microbial communities.

## CHAPTER 3: Materials and Methods

### 3.1 Experimental Design

#### 3.1.1 *Unique Simplex Centroid Model*

This experiment followed a unique simplex centroid mixture design (Figure 3.1) to collect data from different mixtures among the three substrate types: meat waste (MW), fruit and vegetable waste (FVW), and fat, oil, and grease (FOG) waste. The experiment consisted of three stages where reactors were either introduced to a new substrate type or destructively sampled for future microbial community analysis. The loading and sampling schedule is demonstrated in Table 3.1. Eighteen lab-scale reactors were divided equally among the three vertices of the ternary plot, with six starting at each one. Stage one is denoted at each vertex of the ternary plot; reactors were loaded with 100% of that corresponding food waste type. At vertex A, reactors were loaded with 39 g COD of (FVW). The six reactors were loaded with 39 g COD of FOG at vertex C, and meat waste (MW) at vertex B. Loading rate for MW reactors was slightly higher due to COD measurement error, so they were loaded with 53 g COD instead of the planned 39 g COD. Methane generation was monitored throughout the experiment (see below in Chapter 4). Once the methane generation peaked and began to decline, one reactor from each vertex was destructively sampled and frozen at -80 °C until microbial community analysis could be performed.

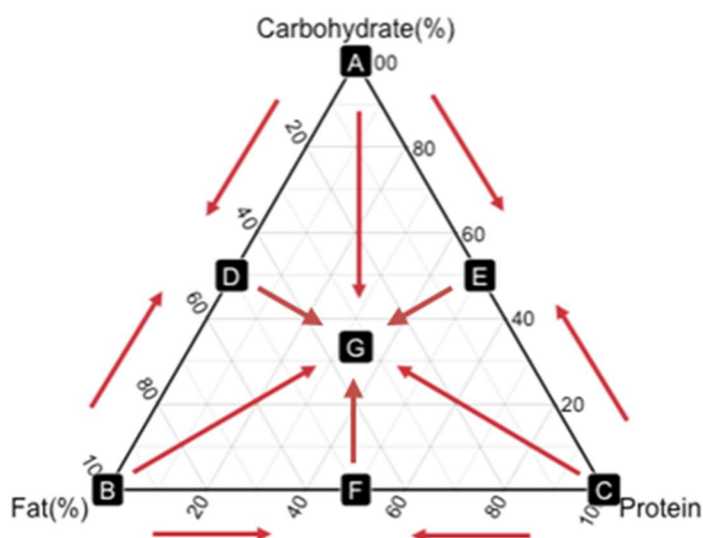


Figure 3.1: Unique simplex centroid model

Table 3.1: Sampling and Loading Schedule

Simplex Centroid Mixture Design: Sampling and Loading Schedule						
Reactor Code	Stage 1		Stage 2		Stage 3	
	Mixture Point	Action on Reactor	Mixture Point	Action on Reactor	Mixture Point	Action on Reactor
R1	A	→	E	Destructively Sampled		
R2	A	→	E	→	G	Destructively Sampled
R3	A	→	G	Destructively Sampled		
R4	A	Destructively Sampled				
R5	A	→	D	→	G	Destructively Sampled
R6	A	→	D	Destructively Sampled		
R7	C	→	F	→	G	Destructively Sampled
R8	C	→	E	→	G	Destructively Sampled
R9	C	Destructively Sampled				
R10	C	→	E	Destructively Sampled		
R11	C	→	F	Destructively Sampled		
R12	C	Destructively Sampled				
R13	B	→	D	→	G	Destructively Sampled
R14	B	Destructively Sampled				
R15	B	→	D	Destructively Sampled		
R16	B	Destructively Sampled				
R17	B	→	F	→	G	Destructively Sampled
R18	B	→	F	Destructively Sampled		

Stage 2 loading occurred once methane generation was close to zero. Figure 2 demonstrates the sampling and loading schedule. In Stage 2, reactors were loaded towards the adjacent middle points connected to the original vertex. The remaining 15 reactors were meant to be loaded towards mixture points D, E, F, and G on the ternary plot. Points D, E, and F are a 50/50 COD-based mixture of a reactor's original substrate type from Stage 1 and a new substrate type. G is equal COD parts of all three substrate types. Due to hypothesized microbial failure in two reactors, these reactors were destructively sampled, and the pathways B to G and C to G were cut from the experiment. The five reactors remaining at point A were split towards either D, E, or G. One reactor was loaded to G, two reactors to D, and two to E. These reactors were loaded with the 50/50 COD-based mixture of FVW and either MW or FOG. The same strategy was used for reactors from vertices B and C. The reactors were divided among the pathways, half towards each adjacent point from the starting vertex.

Again, once methane generation peaked, one reactor from every pathway was destructively sampled for microbial community analysis. This resulted in two reactors from D, two from F, and two from E. When methane generation was nearly zero, Stage 3 was started. The remaining reactors were all loaded towards mixture point G, with equal loading rates of all three substrate types (13 g COD of each substrate).

This method allowed process performance data and microbial community samples to be collected at each mixture point possible within the ternary plot, except for the pathways directly to mixture point G due to early microbial failure.

### 3.1.2 Reactor Design

All reactors were operated under mesophilic conditions (37 °C). The experiment included 21 one-gallon (3.78 l) plastic body reactors (Figure 3.2). Three acted as controls and were fed only inoculum, while 18 were loaded with inoculum and food waste. The reactors had rubber stoppers to close the system to the atmosphere, making the system anaerobic. Reactors were connected to 10 L gas bags (SKC Inc., Eighty Four, PA) using Tygon tubing for gas collection and 2-liter leachate bags to collect and recirculate leachate every three days. The reactors had a working volume of 3 L. At the beginning of each stage, the substrate mixtures were well mixed before loading the reactors. Reactors were flushed with N<sub>2</sub> gas for 15 minutes after each loading to ensure an anaerobic environment.



Figure 3.2: Laboratory set-up at the beginning of Stage 1 of the experiment.

### 3.2 Substrate and Inoculum Composition

Reactors were inoculated with decomposed synthetic municipal solid waste (MSW) collected from a ~300 L drum in the Environmental Engineering (ENE) lab at NC State University. A month prior to collecting from the drum, the drum was loaded with synthetic waste composed of municipal waste collected from NCSU student dorms, shredded paper, and rabbit food. This was to feed the microbial community in the drum and activate gas production. The previously decomposed waste was removed from the drum and mixed thoroughly with the new waste in the ENE lab. The waste was loaded back into the drum to monitor gas production. Once the methane generation peaked and biogas production began to plateau, ~60 L of decomposed waste was collected from the drum to be used as inoculum in the reactors.

The fruits, vegetables, and meat were collected from a local grocery store. The ratios of the type of fruits, vegetables, and meat were calculated based on USDA food loss adjusted data in 2017 (USDA, 2021, Table 3.2 and 3.3). Fruit and vegetable waste were cut into bite-sized pieces, shown in Figures 3.3 and 3.4, respectively. Ground meat was used for protein waste. The meat was cooked on the stovetop without adding oil until cooked through (Figure 3.5).



Figure 3.3: Chopped fruit waste used for carbohydrate waste.



Figure 3.4: Chopped vegetable waste used for carbohydrate waste.



Figure 3.5: Cooked ground meat for the protein waste.

Table 3.2: Composition of carbohydrate waste (wet weight %) based on US loss adjusted food availability data (USDA, 2021)

Carbohydrate Waste			
Fruit Waste		Vegetable Waste	
Apples	17%	Cucumbers	14%
Bananas	43%	Tomatoes	22%
Grapes	9%	Onions	32%
Oranges	15%	Lettuce	19%
Melon	16%	Carrots	12%

Table 3.3: Composition of protein waste (wet weight %) based on US loss adjusted food availability data (USDA, 2021)

Protein Waste	
Beef	31%
Chicken	43%
Pork	26%

Grease interceptor waste (GIW) comprises three layers: fats, oils, grease (FOG), wastewater, and food solids. Grease interceptor waste (GIW) was collected from a local grease trap cleaning service that collects grease trap waste from restaurants in the Raleigh-Durham region. This company renders usable grease from the GIW and sells it as bunker fuel for ships. The remaining wastewater is processed, and food solids are composted. The company provided a

5-gallon bucket of GIW from restaurant waste they had previously collected and stored at their plant but had not yet been processed. Only the fat, oil, and grease (FOG) layer was of interest for this project. A subsample from the bucket was removed to isolate the FOG layer to fill a 2 L jar. The jar was left at room temperature to settle into the three distinct layers: FOG, wastewater, and food particles. After settling, the top layer, FOG, was carefully removed using a serological pipette and transferred to a jar to preserve until reactor loading. This was repeated at each stage. At the end of the experiment, ~3L of FOG had been removed and used for loading. All three substrates were stored at 4°C prior to loading into the reactors.

### **3.3 Data Collection Methods**

#### *3.3.1 Process Performance Data Collection*

All reactors were operated under mesophilic conditions and were manually shaken daily for one minute. Leachate was collected into 2L leachate bags via a connection to the sampling port at the bottom of the reactor. Leachate bags were drained back into the reactors every three days to recirculate the leachate through the system. Leachate volume varied from 100 mL to 300 mL among reactors due to the different water content of the waste types. Gas composition and volume were measured every four to seven days. Biogas volume was measured by evacuating the gas bag into a cylinder of a known volume, and the pressure difference was monitored and normalized to standard temperature and pressure (STP). The composition of the biogas was measured using a gas chromatograph (SRI 8610C, Shimadzu, Columbia, MD) with a thermal conductivity detector (TCD) and a flame ionization detector (FID). When a reactor was destructively sampled or loaded, samples for volatile fatty acids analysis were taken at the end of each stage. VFA samples are kept at 4°C until ready to be processed. VFA concentration (acetic, propionic, butyric, valeric, and hexanoic acids) will be measured through acidification,

centrifugation, filtration, and direct injection into a GC (GC-2014 Shimadzu). Chemical oxygen demand (COD) was measured weekly using high range HACH COD kits (200 to 15,000 mg/L) (HACH Company, Loveland, CO). The pH was measured using Standard Methods (APHA, 2005) and was measured every other day during the start-up period, then reduced to once a week once stabilized. The pH was consistently above the optimal range ( $>7.5$ ), so reactors were neutralized using 2M HCl. Total ammonia concentrations were measured initially at the beginning and end of Stage 1, then increased weekly to monitor changes in ammonia concentration closely. Total ammonia was measured using high range HACH kits, 0 to 50 mg/L (Loveland, CO).

### *3.3.2 DNA: Sample Processing, Extracting, and Sequencing Methods*

Destructively sampled reactors were kept in  $-80^{\circ}\text{C}$  freezers until ready to be processed for DNA extraction. Reactors were allowed to thaw at  $4^{\circ}\text{C}$  before being processed. Samples were processed following the indirect phosphate buffer method developed by Staley et al., 2011. Reactor contents were removed and thoroughly mixed before separating half for processing and half stored at  $-80^{\circ}\text{C}$ . The waste was divided into 50 g aliquots with triplicate aliquots for each reactor. Each aliquot was combined with 250 mL  $\text{PO}_4$  buffer and blended for 1 minute. The blended mixture was then poured and squeezed through a nylon painter strainer bag to separate microbial cells. The supernatant was collected and transferred to sterile tubes to be centrifuged at  $3,220 \times g$  for 5 minutes. DNA was extracted using a DNeasy Powersoil kit following the provided protocol (Qiagen, 2018).

### 3.4 Data Analysis

#### 3.4.1 Statistical Data Analysis

The methane gas production data were analyzed using the statistical analysis provided by NC State statistical consultants (Wood et al., 2021). The consultants provided various models to highlight mixtures that produced the most methane, giving insight into the optimal mixture points in the ternary plot. The analysis was performed in the coding language R. First, an analysis of variance was run in R using a one-way ANOVA function to determine if the results were significant. Then, the Scheffé model was applied at each stage using the appropriate polynomial for the type of data.

Stage 1 mixture design results were analyzed using Scheffé linear model. The linear model for this three-component mixture experiment is modeled as:

$$y = \beta_1 x_1 + \beta_2 x_2 + \beta_3 x_3 + \epsilon \quad (\text{Eq. 3.1})$$

The response variable ( $y$ ) is the methane production,  $x_1, x_2, x_3$  are the proportions of carbohydrate, protein, and fat in a mixture,  $\beta_1, \beta_2, \beta_3$  are the respective parameter estimates for the three substrates, and  $\epsilon$  is the experimental error.

This model is extended to accommodate the interactions between substrate pairs, denoted in equation 3.2. This is the model used to analyze Stage 2 data.  $\beta_{12}, \beta_{23}, \beta_{13}$  are the estimate parameters for the interactions between carbohydrate, lipid, and protein.

$$y = \beta_1 x_1 + \beta_2 x_2 + \beta_3 x_3 + \beta_{12} x_1 x_2 + \beta_{23} x_2 x_3 + \beta_{13} x_3 x_1 \quad (\text{Eq. 3.2})$$

To accommodate for stage 3 interactions, Eq. 3.2 is further expanded to the following.

$$y = \beta_1 x_1 + \beta_2 x_2 + \beta_3 x_3 + \beta_{12} x_1 x_2 + \beta_{23} x_2 x_3 + \beta_{13} x_3 x_1 + \beta_{123} x_1 x_2 x_3 \quad (\text{Eq.3.3})$$

This specific cubic model includes parameter estimates for all possible substrate interactions within this experiment, therefore was used to analyze Stage 3 data.

## CHAPTER 4: Results and Discussion

The objective of this study was to monitor reactor performance and microbial communities after introducing new substrate mixtures at different stages. Biogas production is a reflective parameter of reactor stability as biogas production depends on a balanced and robust microbial community. This section will discuss the biogas production rates and cumulative yields through the duration of the experiment and other chemical parameters such as pH changes and ammonia concentrations.

### 4.1 Loading Rate

The loading rate for each reactor was planned to be 39g COD of substrate (13 gCOD/L). The goal is to have a loading rate that will result in a measurable amount of biogas but not overload the microbial communities in the reactor. Carbohydrate waste typically has the lowest COD per liter of these three substrate types, so was used as the control when deciding the loading rate. Past experiments at NCSU have used a 1:9 substrate to inoculum ratio when loading carbohydrate waste, so this ratio was used to find the COD loading rate. Using the COD concentrations of substrate found in Table 4.1, this ratio resulted in a loading rate of 39 g COD. This loading rate was applied to all substrate types to maintain consistent COD loadings in each reactor.

Table 4.1: Substrate COD concentrations

Substrate COD	gCOD/L	Standard Deviation
FVW	132	21
MW	394	19
FOG	150	11

The loading rate of the protein-based reactors is 53 gCOD due to COD measurement error at the beginning of the experiment. Substrate COD was measured using HACH digestion vial kits. To prepare the substrate for measurement, the meat waste was first blended with deionized water to create a slurry to dilute the COD concentration in the sample and decrease the thickness of the sample to transfer with a pipette. Even after being blended for one minute, the meat waste still had solids that could have impacted the digestion within the COD vials. The solids could have affected the spectrometry reading since they will block light. Additionally, the protein waste was measured using the slurry method without serial dilution. The protein waste was heavily diluted and blended. In Stage 3, when additional protein waste needed to be collected and measured, the new protein waste was measured to check the COD before loading. The protein waste was mixed with deionized water enough to make it transferable, but then a serial dilution method with triplicates was used, and a more accurate COD concentration was found. This error was adjusted for in Stage 3 by changing the volume of meat waste loaded, but Stage 1 and 2 reactors loaded with protein have a higher COD loading rate. These plots were normalized by the correct COD (Table 4.1) to allow for comparison between reactors.

For the lipids, grease waste is notoriously challenging to characterize and often results in a large standard error in COD measurements. The COD was measured using a careful serial dilution method and five replicates. The COD of FOG was lower than expected. This could be attributed to the source of GIW as it was collected from a treatment facility, not directly from a grease trap. This collected GIW could have already gone through preliminary treatment steps before separating the FOG, wastewater, and food solids. This could have resulted in lower COD concentrations. Additionally, as mentioned in Chapter 3, the FOG was separated by allowing the wastewater and food particle layers to settle out. FOG was stored in a separate container until

ready to load into the reactors, allowing for more time remaining wastewater to settle out. Loading volumes were drawn from this more concentrated FOG, potentially resulting in an increased COD concentration and subsequently, an increased loading rate. Therefore, all methane graphs are normalized by gCOD<sub>added</sub> to allow for accurate comparison.

## 4.2 Stage 1 Results

At the start of the experiment, 18 reactors (R1-R18) were loaded with a single type of food waste. Reactors R1 through R6 were loaded with carbohydrate waste, R7 through R12 were loaded with proteinaceous waste, and R13 through R18 was loaded with lipid waste. Table 4.2 summarizes the initial loading volumes for the inoculum and substrate types.

Table 4.2: Stage 1 Inoculum and Substrate Loading Rates

Reactor Code	Inoculum	Substrate	Mixture Point	Volume of Mixture (L)	Volume of Inoculum (L)	Volume of Food Waste (L)	Substrate Loading (g COD)
R1	Solid Waste	FVW	A	3.0	2.7	0.3	39.0
R2	Solid Waste	FVW	A	3.0	2.7	0.3	39.0
R3	Solid Waste	FVW	A	3.0	2.7	0.3	39.0
R4	Solid Waste	FVW	A	3.0	2.7	0.3	39.0
R5	Solid Waste	FVW	A	3.0	2.7	0.3	39.0
R6	Solid Waste	FVW	A	3.0	2.7	0.3	39.0
R7	Solid Waste	MW	C	2.8	2.7	0.1	53.0
R8	Solid Waste	MW	C	2.8	2.7	0.1	53.0
R9	Solid Waste	MW	C	2.8	2.7	0.1	53.0
R10	Solid Waste	MW	C	2.8	2.7	0.1	53.0
R11	Solid Waste	MW	C	2.8	2.7	0.1	53.0
R12	Solid Waste	MW	C	2.8	2.7	0.1	53.0
R13	Solid Waste	FOG	B	3.0	2.7	0.3	39.0
R14	Solid Waste	FOG	B	3.0	2.7	0.3	39.0
R15	Solid Waste	FOG	B	3.0	2.7	0.3	39.0
R16	Solid Waste	FOG	B	3.0	2.7	0.3	39.0
R17	Solid Waste	FOG	B	3.0	2.7	0.3	39.0
R18	Solid Waste	FOG	B	3.0	2.7	0.3	39.0
C1/R19	Solid Waste	Control		2.7	2.7	0.0	N/A
C2/R20	Solid Waste	Control		2.7	2.7	0.0	N/A
C3/R21	Solid Waste	Control		2.7	2.7	0.0	N/A

FVW: Fruit and Vegetable Waste; MW: Meat Waste; FOG: Fats, Oil, and Grease

#### 4.2.1 Methane Generation Data

All methane data presented in this section has been corrected for methane attributed to the inoculum, assuming that the methane production from the inoculum was the same in the control and treatment reactors. The average methane volume from the control reactors was subtracted from each reactor for each gas measurement. Methane volume was calculated by multiplying the measured biogas volume by the percent of methane measured using gas chromatography. The production rates were then calculated by dividing the volume of methane by the number of days since the last loading and then by the amount of COD added to the reactor at the previous loading ( $\text{mL CH}_4/\text{day}/\text{g COD}_{\text{added}}$ ).

The Stage 1 methane production rates are presented in Figure 4.1 from Stage 1. The pink plots represented the protein-based reactors with the highest average production rates. For protein-based reactors, the highest peak production rate was achieved by R7, reaching 17 mL  $\text{CH}_4/\text{g COD}_{\text{added}}$ .

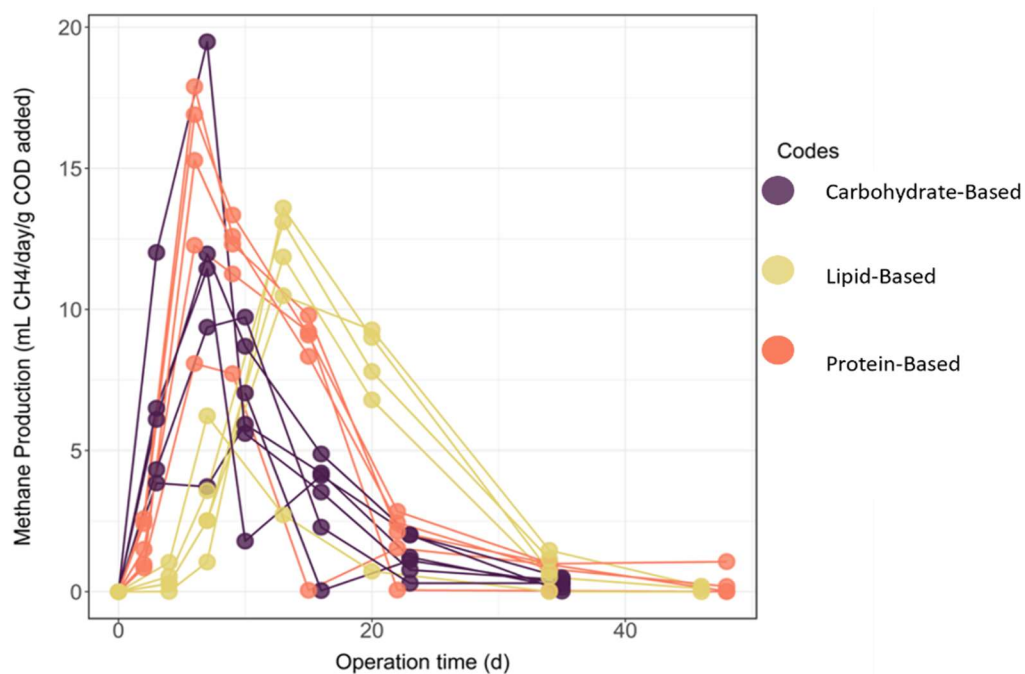


Figure 4.1 Methane Production Rates for Stage 1 grouped as substrate types

Cumulative methane was also calculated from the biogas data to understand the total yield from each reactor. The volumes of methane were normalized by the amount of COD loaded into the reactor to allow comparison between the reactors. Figure 4.2 displays the cumulative methane from each reactor to compare among substrate type. These reactors are replicates at this stage, so the averages are plotted in Figure 4.3. Figures 4.4 through 4.6 display the methane yields from each reactor to compare individual reactors.

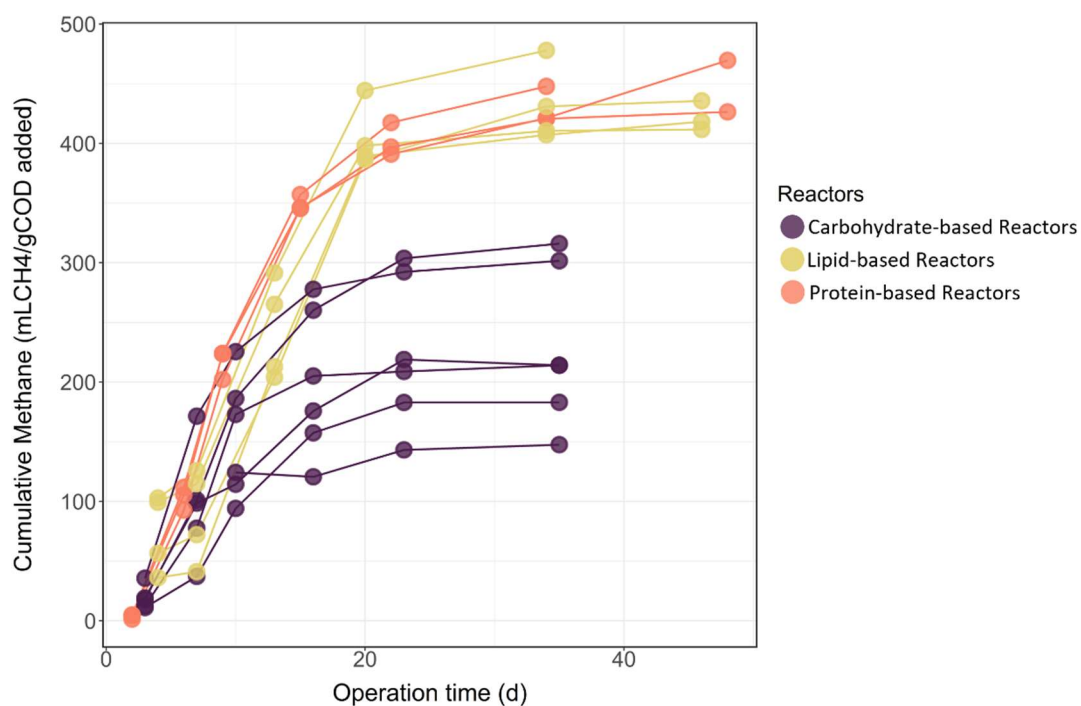


Figure 4.2: Cumulative Methane yield during Stage 1 from all reactors grouped as substrate-based from loading in stage 1

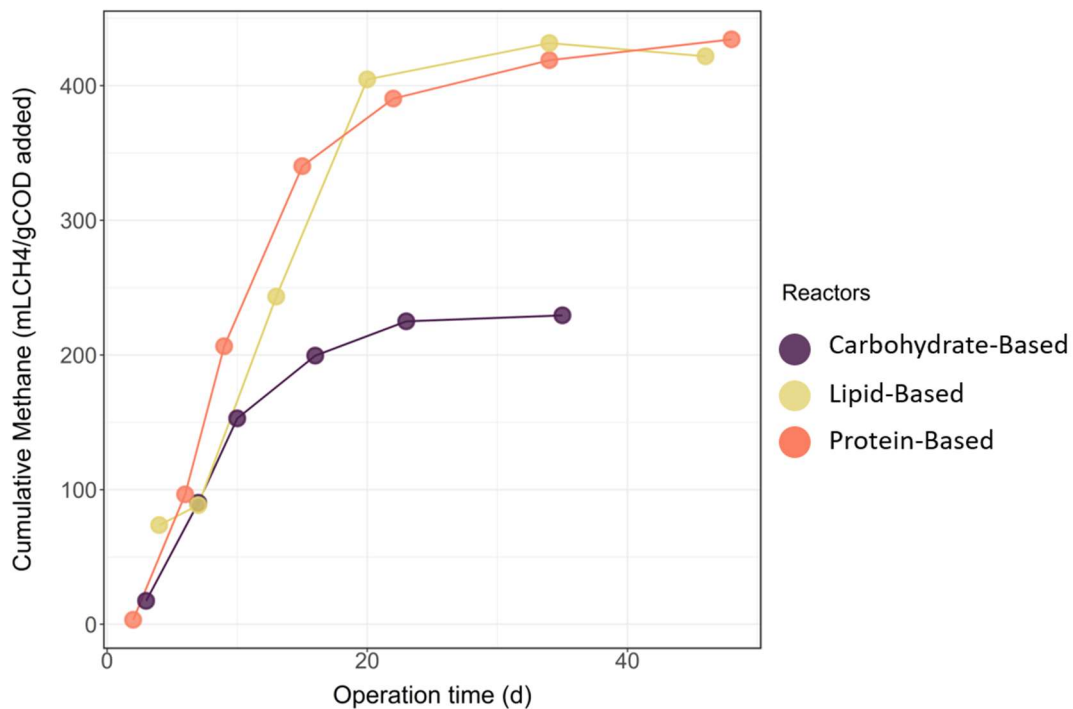


Figure 4.3: Average cumulative methane yield from replicate reactors in Stage 1

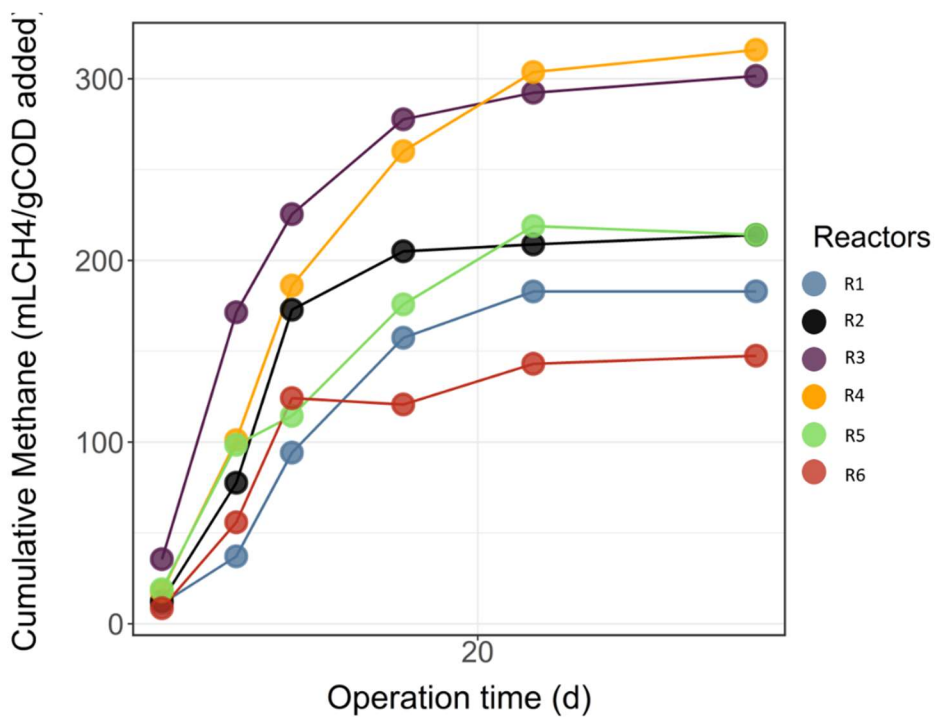


Figure 4.4: Cumulative methane yields from Stage 1 from Carbohydrate-based reactors

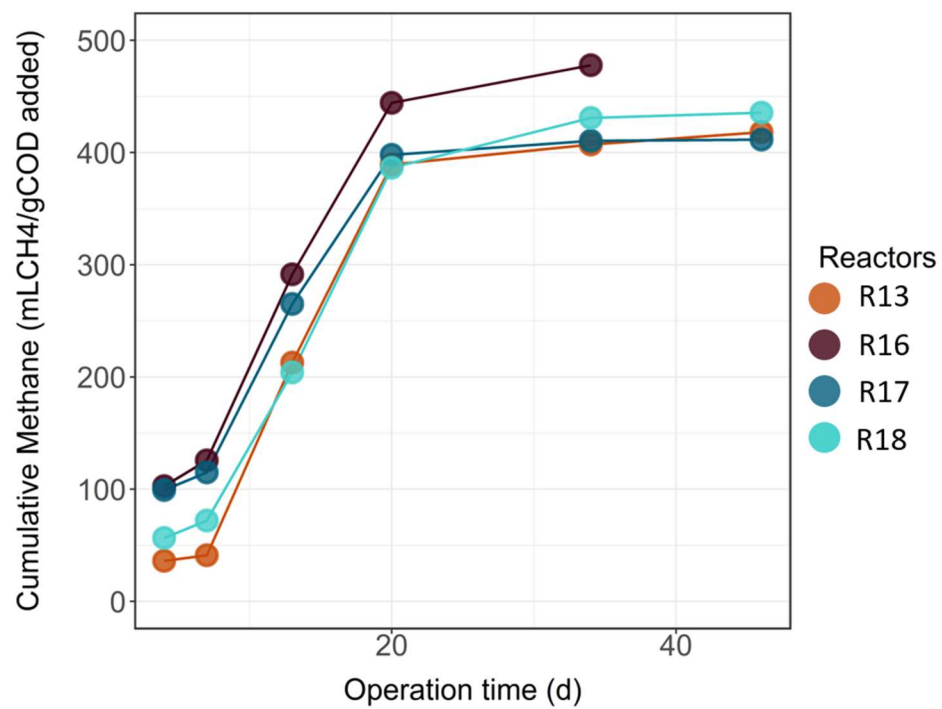


Figure 4.5: Cumulative methane yields from Stage 1 from Lipid-based reactors

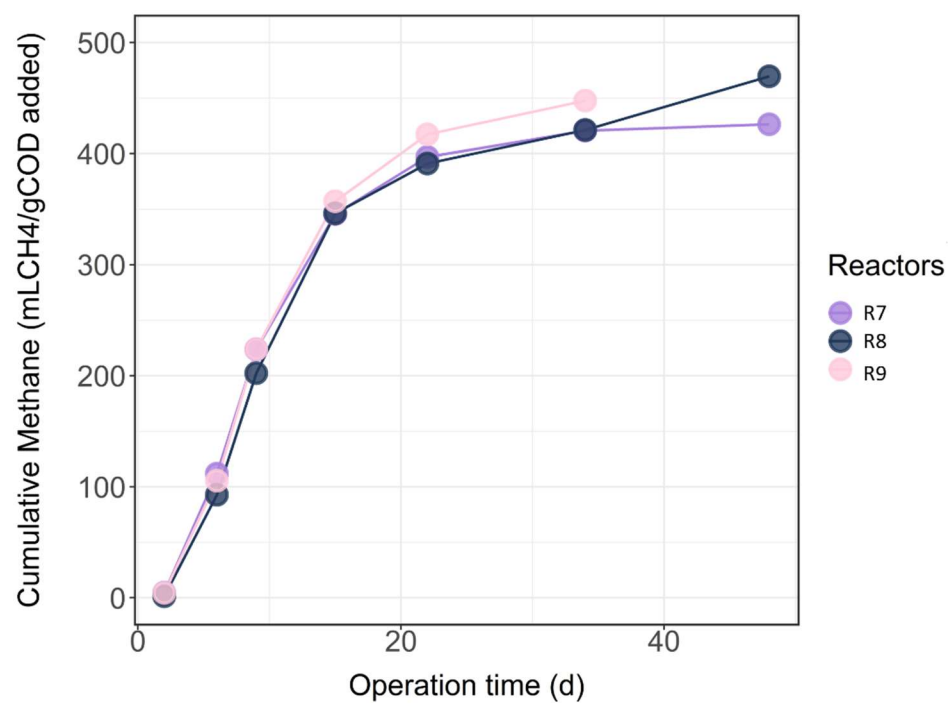


Figure 4.6: Cumulative methane yields from Stage 1 from Protein-based reactors

Once methane production and cumulative methane stabilized, one reactor from each mixture point (A, B, and C) was destructively sampled. Reactors R4, R9, and R16 were randomly chosen to be removed at the end of stage 1. R12 and R14 were also destructively sampled due to deficient gas production. Headspace samples from these reactors were collected and analyzed to investigate potential leaks. Oxygen gas concentration was less than 2%, and methane content was ~15% in both reactors, so it is hypothesized this low gas production is due to early microbial failure of the community in the inoculum. The remaining reactors were monitored until gas production was nearly zero.

#### 4.2.2 Ammonia concentrations in the reactors

Ammonia and COD concentration were measured from leachate samples at the beginning and end of stage Stage 1. These concentrations and the resulting COD/NH<sub>3</sub> ratio are summarized in Table 4.3.

Table 4.3: Ammonia and COD concentrations beginning and end of Stage 1. The number in parenthesis on the ammonia concentrations represents the pH of the samples.

Mixture Point	Substrate Description	Reactor Code	Start of Stage 1			End of Stage 1			% Change in COD
			(mg NH <sub>3</sub> - N/L)	(g COD/L)	COD/N H <sub>3</sub>	(mg NH <sub>3</sub> - N/L)	(g COD/L)	COD/N H <sub>3</sub>	
A	FVW	R1	520 (7.95)	10	19.2	1790 (7.81)	6.8	3.8	-32.0
A	FVW	R2	1230 (7.87)	8.4	5.5	1680 (7.87)	6.8	5.0	-19.0
A	FVW	R3	1370 (7.95)	14.1	10.3	1460 (7.85)	6.1	4.2	-56.7
A	FVW	R4	1230 (7.01)	18.7	15.2	1330 (7.7)	7.7	6.4	-58.8
A	FVW	R5	1390 (7.86)	11.5	8.3	1210 (7.75)	5.3	4.4	-53.9
A	FVW	R6	1370 (7.85)	10	7.3	1120 (7.7)	6.4	5.7	-36.0
C	MW	R7	3870 (8.14)	15.1	3.9	4260 (8.04)	10	2.3	-33.8
C	MW	R8	3900 (8.18)	15.7	4.0	4380 (8.02)	11.8	2.7	-24.8
C	MW	R9	1540 (8.14)	13.7	8.9	5000 (8.00)	9.1	1.8	-33.6
C	MW	R10	4620 (8.16)	24.7	5.3	4900 (8.02)	12.7	2.6	-48.6
C	MW	R11	3980 (8.17)	25.4	3.4	5080 (8.11)	13.7	5.0	.46.1
C	MW	R12	3900 (8.21)	19.9	5.1	1100 (8.17)	10.7	9.7	-46.2
B	FOG	R13	1140 (7.72)	12.6	8.1	1140 (7.83)	9.2	11.1	-27.0
B	FOG	R14	910 (7.76)	11.7	37.7	1010 (7.85)	7	7.0	-40.2
B	FOG	R15	1180 (7.61)	17.9	15.2	1030 (7.78)	8.8	8.5	-50.8
B	FOG	R16	1090 (7.19)	26.1	23.9	1110 (7.32)	8.8	7.9	-66.3
B	FOG	R17	990 (7.66)	14.1	14.2	1290 (7.58)	10.1	7.8	-28.4
B	FOG	R18	1090 (7.44)	18.4	16.9	1130 (7.41)	10.4	9.2	-43.5

### 4.2.3 Stage 1 Discussion

In Stage 1, the protein-based reactors collectively have the highest peak production rates in Stage 1. Both protein and carbohydrate-based reactors reached peak production after ten days from the first loading. Lipid-based reactors took slightly longer, peaking at around 15 days. Lipids are harder for hydrolytic microbes to ferment into smaller acids due to their complicated structure, so this slight lag phase is expected.

An essential parameter for AcD is the carbon to nitrogen (C/N) ratio, and is considered optimal at 20 (Pramanik et al., 2019). This study measured only COD and  $\text{NH}_3$ , so the COD/ $\text{NH}_3$  is a partial estimate of the C/N. For stage 1, these ratios are summarized in Table 4.2. Protein-based reactors had high ammonia concentrations from the beginning. This was expected due to the high nitrogen content of protein waste. This results in a lower C/N ratio in the protein reactors. COD/ $\text{NH}_3$  ratios decreased throughout Stage 1 as COD values decreased, and  $\text{NH}_3$  increased since more ammonia accumulated. The ratios are lowest in C (100% protein) reactors due to the high ammonia concentrations. B (100% lipid) reactors have the largest shift in COD/ $\text{NH}_3$  at the end of Stage 1. Lipid-based reactors showed the largest changes in COD by the end of Stage 1, explaining the highest cumulative yields.

The variability in yields from the carbohydrate-based reactors seen in Figure 4.1 can be explained by the COD/ $\text{NH}_3$  ratios. R3 and R4 had higher COD concentrations in the leachate at the beginning of stage 1 but had similar COD/ $\text{NH}_3$  ratios by the end to the other reactors, showing they had more COD destruction and subsequently more biogas produced. Reactors R1, R2, and R6 had a smaller percent change in COD concentration, suggesting less COD destruction, matching the lower biogas production values than R3 and R4.

Carbohydrate-based reactors did not exceed 350 mL CH<sub>4</sub>, while the protein and lipid-based reactors did exceed 350 mL CH<sub>4</sub>. Errors with the COD concentration explained at the beginning of this chapter could explain the overestimated cumulative yields at the end of stage 1. Nonetheless, it is expected for carbohydrate to produce less methane than protein and lipid as it has the lowest methane potential value (Wang et al., 2018). Cumulative yields at Stage 1 should be the same within each category of waste type as there were loaded with the same COD.

### 4.3 Stage 2 Results

Five reactors were removed from Stage 1, and the remaining reactors were introduced to a new substrate type. Table 4.4 summarizes the Stage 2 loading rates with the type and volume of substrates loaded to each remaining reactor. Stage 2 was longer than Stage 1, lasting over 40 days compared to the 30 days in Stage 1. Stage 2 loading maintained the same loading rate of 39g COD, except the loading rate is divided equally among the different substrates in the mixture. For example, the mixture points D, E and F are a 50/50 mixture on a COD basis, so 19.5 gCOD of each substrate.

Table 4.4: Stage two loaded food waste types and volumes

Reactor Code	Mixture Point	Substrate 1	Volume of Substrate 1 (mL)	Substrate 2	Volume of Substrate 2	Substrate 3	Volume of Substrate 3	Total Volume of Food waste (mL)
R1	A->E	FVW	150	MW	67	N/A	N/A	217
R2	A->E	FVW	150	MW	67	N/A	N/A	217
R3	A->G	FVW	100	MW	45.0	FOG	90	235.0
R5	A->D	FVW	150	FOG	134.0	N/A	N/A	284.0
R6	A->D	FVW	150	FOG	134	N/A	N/A	284
R7	C->F	MW	125	FOG	134.0	N/A	N/A	259.0
R8	C->E	MW	125	FVW	150.0	N/A	N/A	275.0
R10	C->E	MW	125	FVW	150.0	N/A	N/A	275.0
R11	C->F	MW	125	FOG	134	N/A	N/A	259
R13	B->D	FOG	134	FVW	150.0	N/A	N/A	284.0
R15	B->D	FOG	134	FVW	150.0	N/A	N/A	284.0
R17	B->D	FOG	134	MW	125.0	N/A	N/A	259.0
R18	B->D	FOG	134	MW	125	N/A	N/A	259

### 4.3.1 Methane Generation Results

The peak methane production rates occurred quickly, occurring at the first gas collection and measurement point after loading. Figure 4.7 presents the methane production rates in Stage 2. Carbohydrate-based reactors were loaded earlier than lipid and protein-based reactors, demonstrated by the dashed red line. The blue dashed line denotes the loading time for the remaining reactors. All of the reactors experienced a drop in peak production rates in Stage 2. Overall, protein-based reactors had the most significant reduction in production rates.

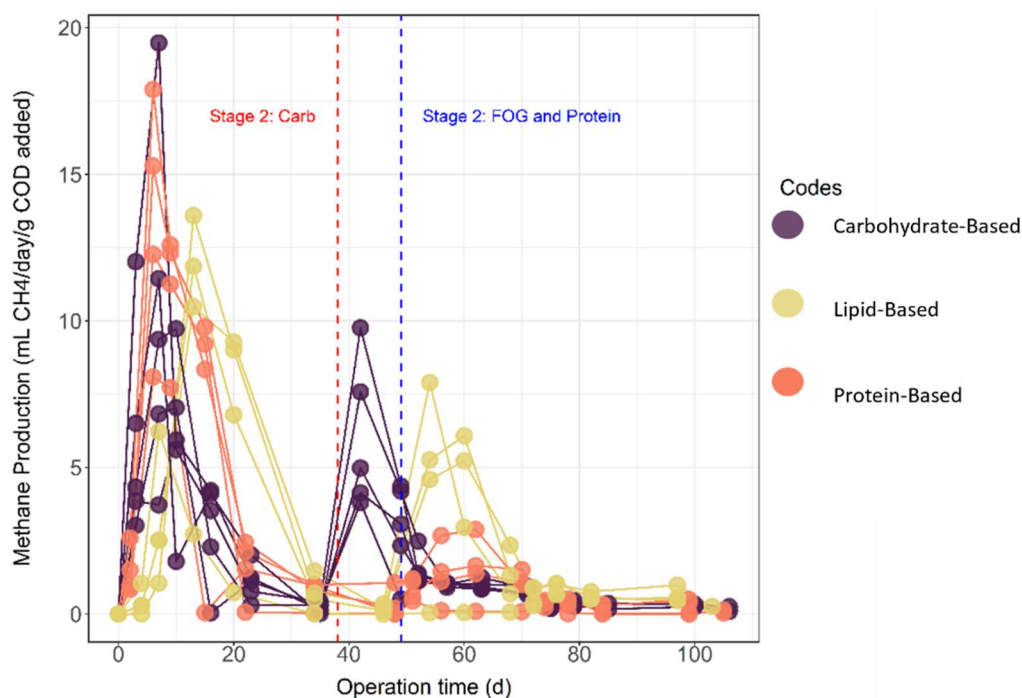


Figure 4.7: Methane production rates in Stage 2.

Cumulative yields through stages 1 and 2 are introduced in figure 4.8. The average yields from replicate reactors are compared in Figure 4.9 to compare the yields from different combinations of waste types. The yields from carbohydrate, lipid, and protein-based reactors are plotted separately in Figures 4.10 through 4.12. The results are further analyzed in Section 4.4.

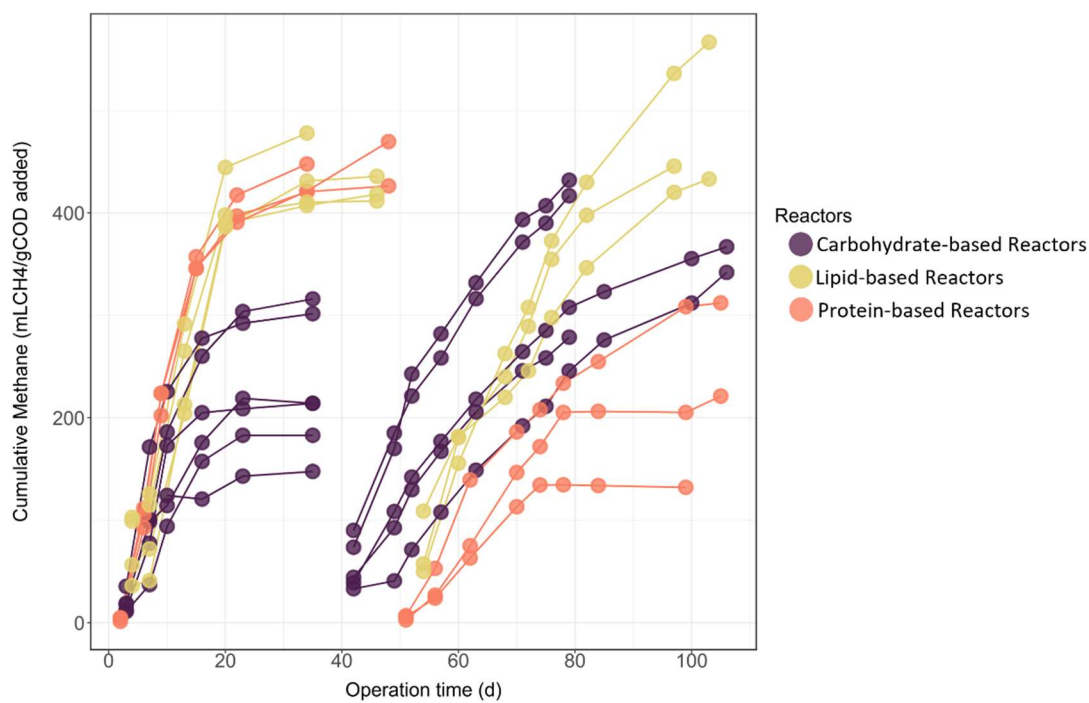


Figure 4.8: Cumulative methane yields from different substrate-based reactors in Stage 2

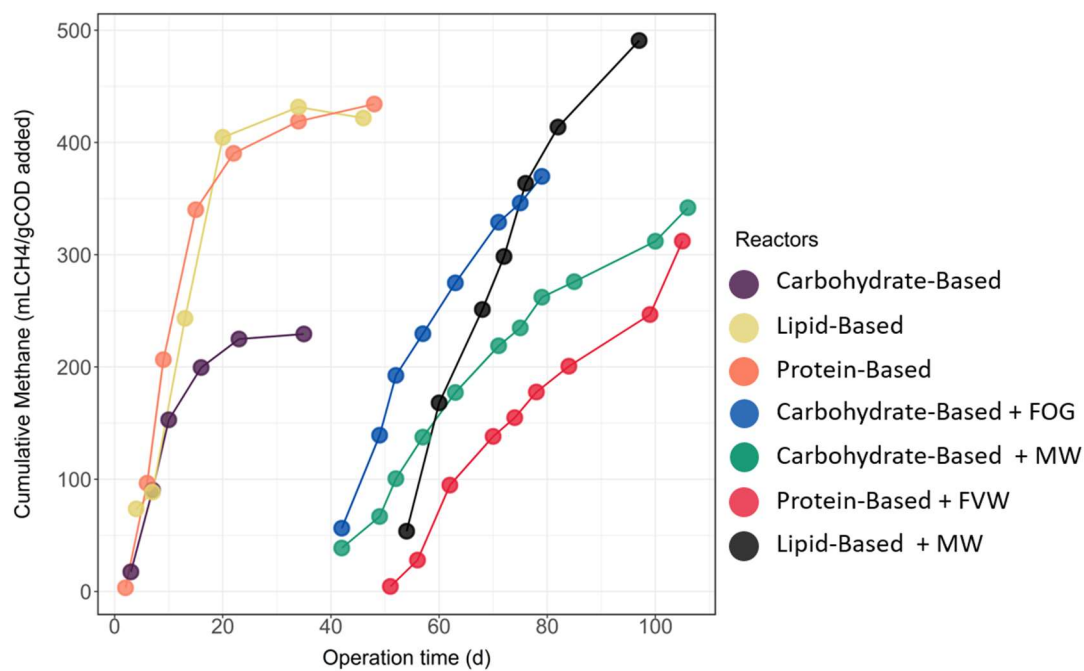


Figure 4.9: Average Cumulative methane yields from replicate reactors at Stage 2

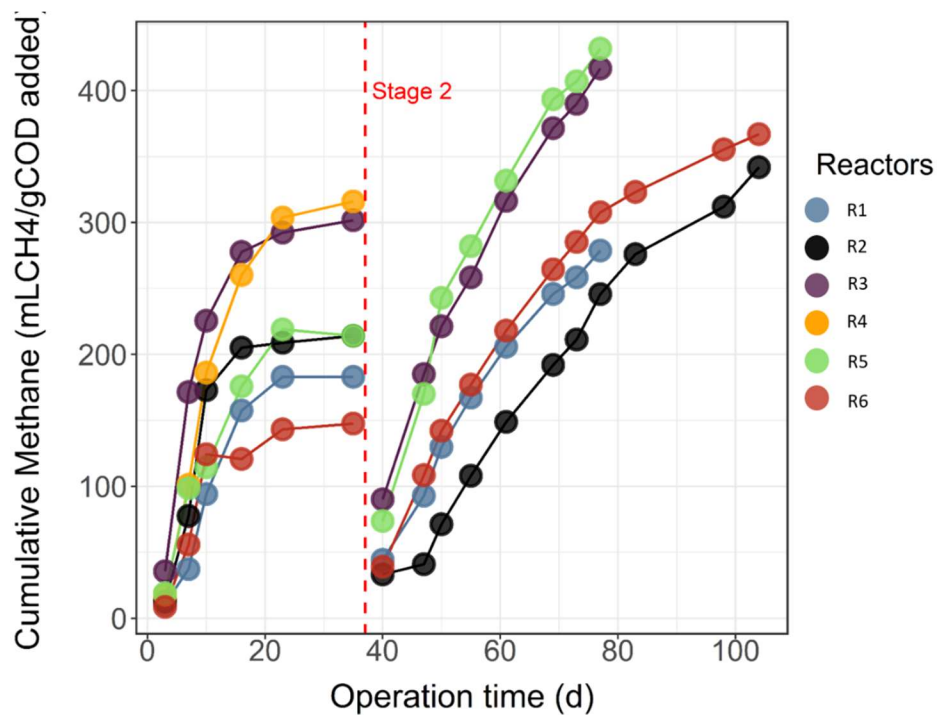


Figure 4.10: Cumulative methane yields during Stage 2 from Carbohydrate-based reactors

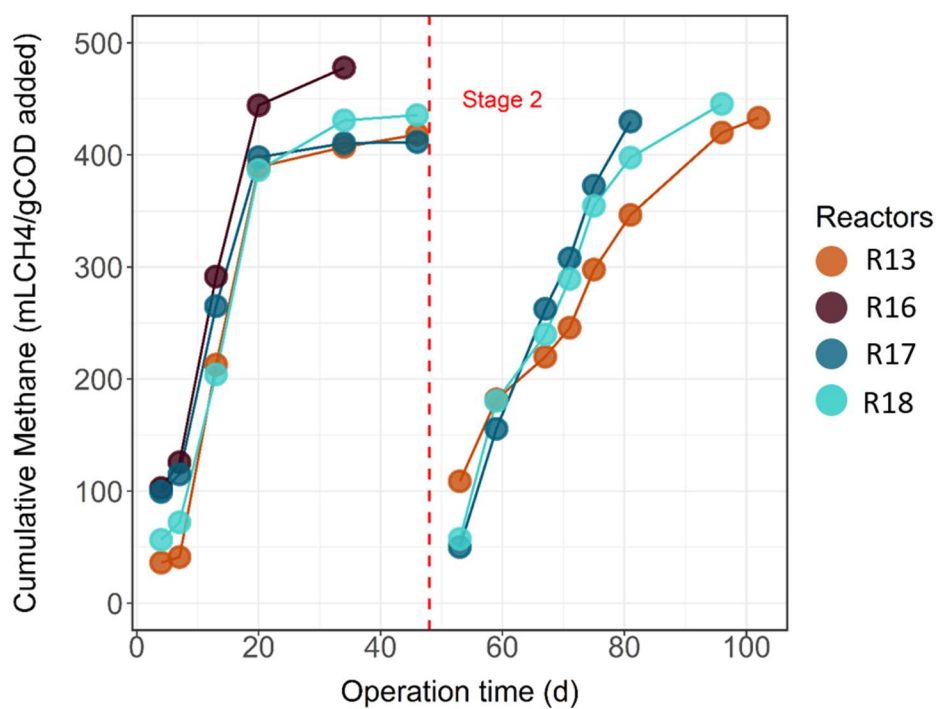


Figure 4.11: Cumulative methane yields during Stage 2 from Lipid-based reactors

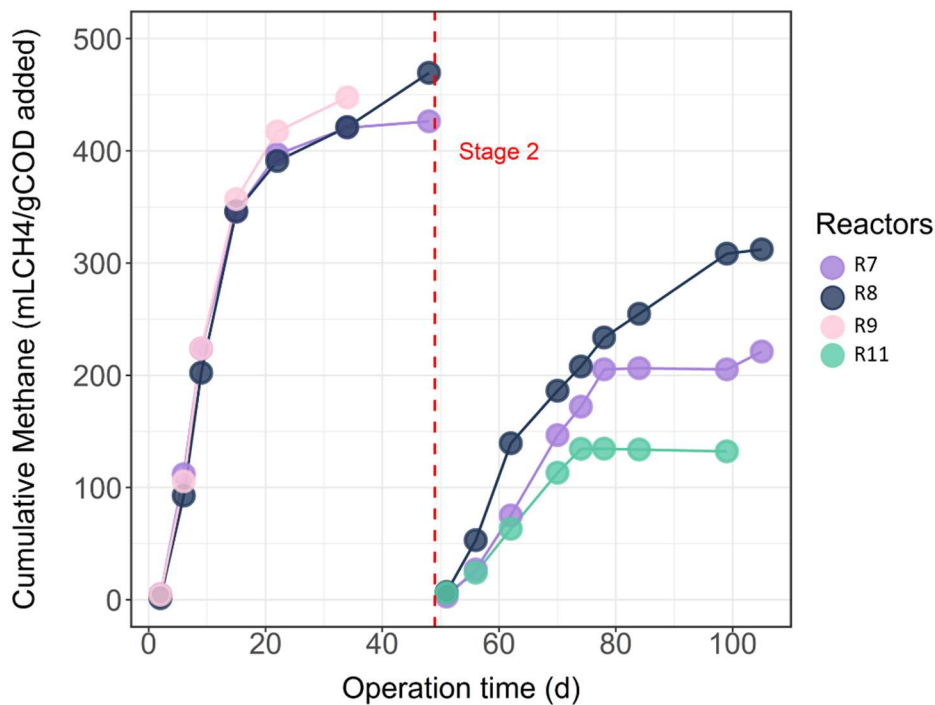


Figure 4.12: Cumulative methane yields during Stage 2 from Protein-based reactors

#### 4.3.2 Ammonia Data

The frequency of ammonia concentration measurements was increased weekly instead of at the beginning and end of the stage to monitor the ammonia concentration in reactors closely. Due to the high ammonia concentrations in protein-based reactors in Stage 1, closer monitoring was required to observe potential inhibition from increasing ammonia concentrations. Table 4.5 summarizes the ammonia concentrations at the beginning and end of Stage 2. The ammonia concentrations throughout the experiment can be found in the Appendix.

Table 4.5: Ammonia and COD concentrations at the start and end of Stage 2. The number in parenthesis on the ammonia concentrations represents the pH of the samples.

Mixture Point	Substrate	Reactor Code	Start of Stage 2			End of Stage 2			% Change in COD
			(mg NH <sub>3</sub> - (pH))	(g COD/ L)	COD/N H <sub>3</sub>	(mg NH <sub>3</sub> - N/L)	(g COD/ L)	COD/N H <sub>3</sub>	
A->E	FVW + MW	R1	2100 (7.69)	16	5.0	2360 (7.81)	10.5	4.4	-34.4
A->E	FVW + MW	R2	1820 (7.82)	26.8	3.4	2430 (7.91)	7.2	3.0	-73.1
A->G	FVW + MW+FOG	R3	1580 (7.91)	13.2	6.3	1680 (7.89)	8.3	4.9	-37.1
A->D	FOG+FVW	R5	1210 (7.84)	10.1	5.6	1190 (7.72)	8.7	7.3	-13.9
A->D	FOG+FVW	R6	1120 (7.72)	6.9	7.8	1240 (7.65)	6.6	5.3	-4.3
C->F	MW + FOG	R7	4100 (8.21)	16.4	4.0	5100 (8.18)	11.8	2.3	-28.0
C->E	MW+FVW	R8	4100 (8.12)	16.6	3.6	6000 (8.20)	14.8	2.8	-10.8
C->E	MW + FVW	R10	4800 (8.15)	16.2	2.6	6700 (8.2)	12.3	2.4	-24.1
C->F	MW + FOG	R11	4800 (8.1)	21.7	4.5	5800 (8.18)	18.3	3.2	-15.7
B->D	FOG+FVW	R13	1130 (7.65)	10.5	9.3	1200 (7.65)	9.2	7.7	-12.4
B->D	FOG + FVW	R15	980 (7.75)	10.3	10.5	1050 (7.61)	6.7	6.4	-35.0
B->F	FOG + MW	R17	1370 (7.66)	11.1	8.1	2730 (7.9)	9.4	3.4	-15.3
B->F	FOG + MW	R18	1600 (7.58)	10.4	6.5	2940 (7.4)	9.7	3.3	-6.7

#### 4.3.3: Stage 2 Discussion

The methane generation peaks occurred faster in Stage 2 than in Stage 1, possibly due to an acclimated microbial community to the substrate types. As seen in Figure 4.7, the protein-based reactors experience a decrease in methane production rates in this stage after being introduced to new substrate types. This shift suggests that the pre-existing microbial communities in the protein-based reactors could not adjust to the difference in the substrate. The genera *Clostridium*, *Proteus*, *Peptococcus*, *Vibrio*, *Bacteroides*, and *Bacillus* are the respective bacterial groups engaged in the hydrolysis of protein waste (Pramanik et al., 2019). While *Clostridium* and *Bacteroides* are also observed in the hydrolysis of carbohydrate and lipid waste, these process performance data suggest that the remaining fermentative microbes can not utilize carbohydrate or lipid waste, so are protein-specific. Specific communities can also convert amino acids from protein degradation to volatile fatty acids and alcohols. *Lactobacillus*, *Escherichia*, *Staphylococcus*, *Micrococcus*, *Bacillus*, *Sarcina*, *Veillonella*, *Pseudomonas*, *Desulfovibrio*, *Desulfuron hydrolysismonas*, *Desulfobacter*, *Selenomonas*, *Streptococcus* all have the metabolic

capability to convert protein to amino acids during acidogenesis (Pramanik et al., 2019). The influence of other substrate types on these microbial communities has not been studied, so the microbial community analysis on the reactors will provide insight into how these protein-specific communities shifted after being introduced to lipid or carbohydrate waste. From the shifts in cumulative production and production rates, it is hypothesized that these communities could not utilize this substrate to the same extent in Stage 1.

Protein degradation results in high ammonia concentrations, as seen in Table 4.5. Protein-based reactors continued to experience an ammonia concentration increase. The reactors originally at mixture point A (FVW) and B (FOG) introduced to protein also saw an increase in ammonia concentration from Stage 1. The threshold stated by McCarty (1964) is 3000 mgNH<sub>3</sub>-N/L, which all the protein-based reactors exceeded. Ammonia concentrations are not inhibitory at these concentrations if pH is adjusted to neutral to decrease ammonia (NH<sub>3</sub>) concentration which is more toxic than ammonium (NH<sub>4</sub><sup>+</sup>) (McCarty, 1964; Syaichurrozi et al., 2013). Therefore, throughout Stage 2, the pH of the reactors was neutralized to 7 using 2M HCl to decrease the pH.

Methanogens are susceptible to high ammonia concentrations, so the concentrations present at this stage could have still impacted the methanogens in the protein-based reactors. While there are contradictory results regarding whether acetoclastic or hydrogenotrophic methanogens are more susceptible, it is generally agreed that syntrophic acetate oxidation (SAO) coupled with hydrogenotrophic methanogenesis is the favored pathway for methane generation at high ammonia concentrations (Ye Chen et al., 2008; Westerholm et al., 2016). *Clostridium* is one of the bacterial groups that can perform SAO under high ammonia (Westerholm et al., 2016). *Methanosarcina* have also been found to tolerate high levels of ammonia, at levels higher than *Methanosaeta* can tolerate (Zhang et al., 2021). *Methanosarcina* have been found able to survive in low C/N ratios,

which are observed in this stage in Table 4.5. Due to the high ammonia concentrations and the limited pathways for methane generation, it is possible the decrease in methane production from protein-based reactors could be a result of limited methanogenesis pathways.

While the production rates in lipid- and carbohydrate-based reactors slightly decreased, they could adapt to the new substrate, including protein. Even when introduced to protein waste, the carbohydrate and lipid-based reactors stayed below the ammonia threshold but had a decrease in COD/NH<sub>3</sub> ratios. This is important to understand so that when full-scale plants decide which food waste to use to start up new digesters, communities formed in protein-fed systems are potentially less resilient to other substrate types than communities in lipid and carbohydrate systems. The microbial communities in the lipid or carbohydrate-fed reactors may be more robust to substrate changes or may be able to utilize a diverse range of substrate types. There is some overlap in microbial communities that can degrade both carbohydrates and lipid waste, such as *Clostridium* and *Staphylococcus*, which could explain the ability of these reactors to adjust well to a mixture of FVW and FOG. Cumulative yield increased in carbohydrate reactors from the addition of either lipid or protein, suggesting that added substrate was beneficial for optimizing methane production and that the microbial communities could adjust to both types of food waste. The COD/NH<sub>3</sub> ratio in carbohydrate-based reactors is lower than the optimal range of C/N (20) and is lower than the values at the end of stage 1.

#### **4.4 Stage 3 Results**

At the end of Stage 2, seven reactors were destructively sampled. The remaining six reactors were loaded to mixture point G, which is all three substrates loaded at equal COD concentrations, ~13 g COD of each substrate type. Table 4.6 summarizes these loading volumes for each reactor.

Table 4.6: Stage 3 loading volumes

Reactor Code	Mixture Point	Substrate 1	Volume of Substrate 1 (mL)	Substrate 2	Volume of Substrate 2 (mL)	Substrate 3	Volume of Substrate 3 (mL)	Total Volume of Food waste (mL)
R2	A-> E-> G	FVW	100	MW	35	FOG	90	225
R6	A-> D-> G	FVW	100	MW	33	FOG	90	223
R7	C-> F-> G	FVW	100	MW	33.0	FOG	90	223
R8	C-> E-> G	FVW	100	MW	33.0	FOG	90	223
R13	B-> D-> G	FVW	100	MW	33.0	FOG	90	223.0
R17	B-> F-> G	FVW	100	MW	33.0	FOG	90	223.0

#### 4.4.1 Methane Generation Data

Stage 3 was the shortest, lasting for 20 days. Figure 4.13 displays the methane production rates for Stage 3, showing a further decrease in peak production rates. Protein production rates were similar to those in Stage 2.

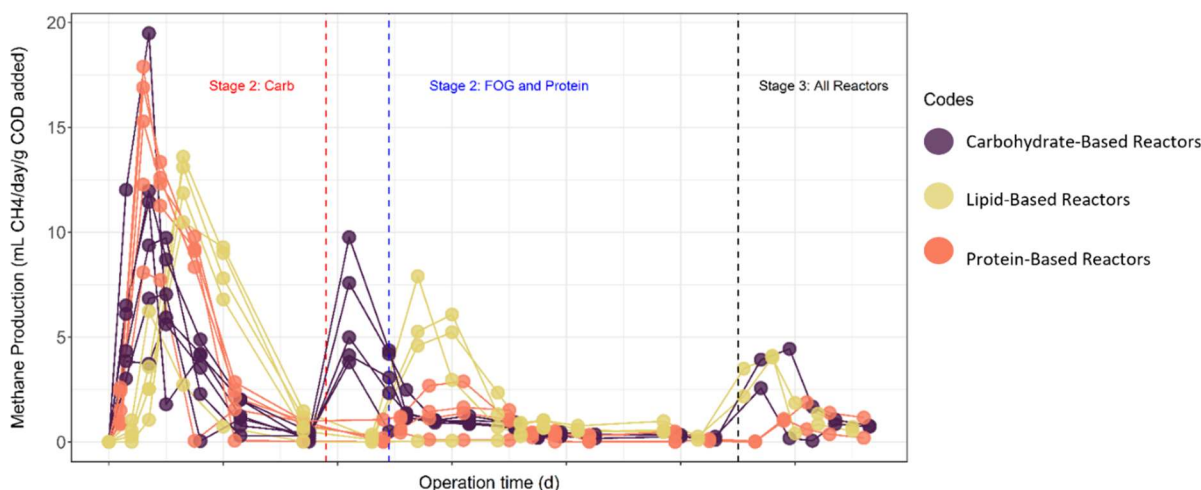


Figure 4.13: Methane production rates in Stage 3.

Cumulative methane throughout the experiment is presented in Figure 4.14. Reactors were destructively sampled after the methane production peaked instead of waiting for cumulative yield to plateau. This allowed microbial community analysis to be performed while the community was near the peak. The yields for carbohydrate, lipid and protein-based reactors are plotted separately in Figures 4.15 through 4.17 respectively.

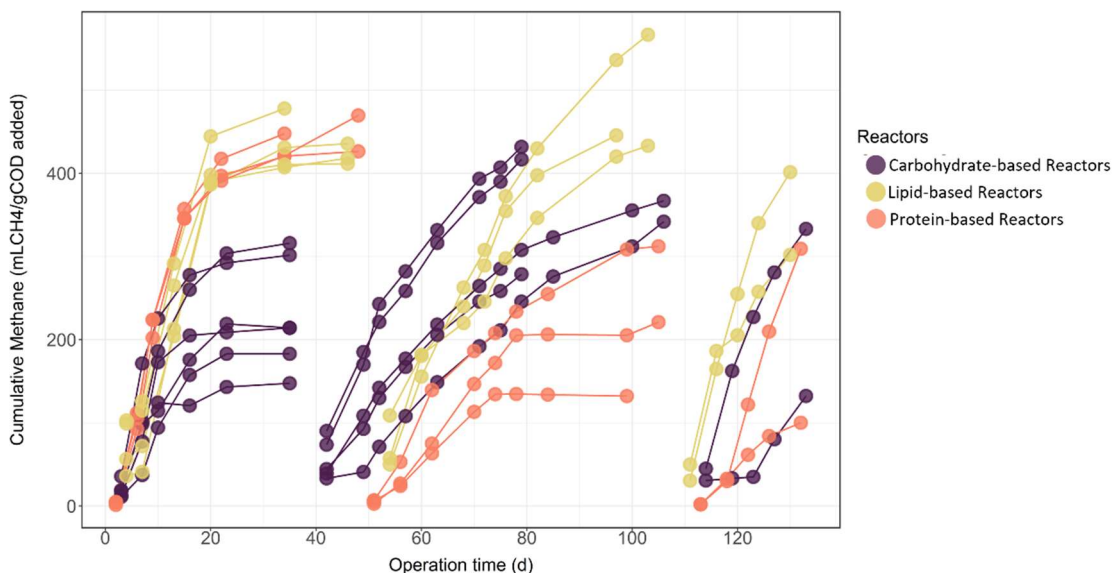


Figure 4.14: Cumulative Methane from the different substrate-based reactors in Stage 3

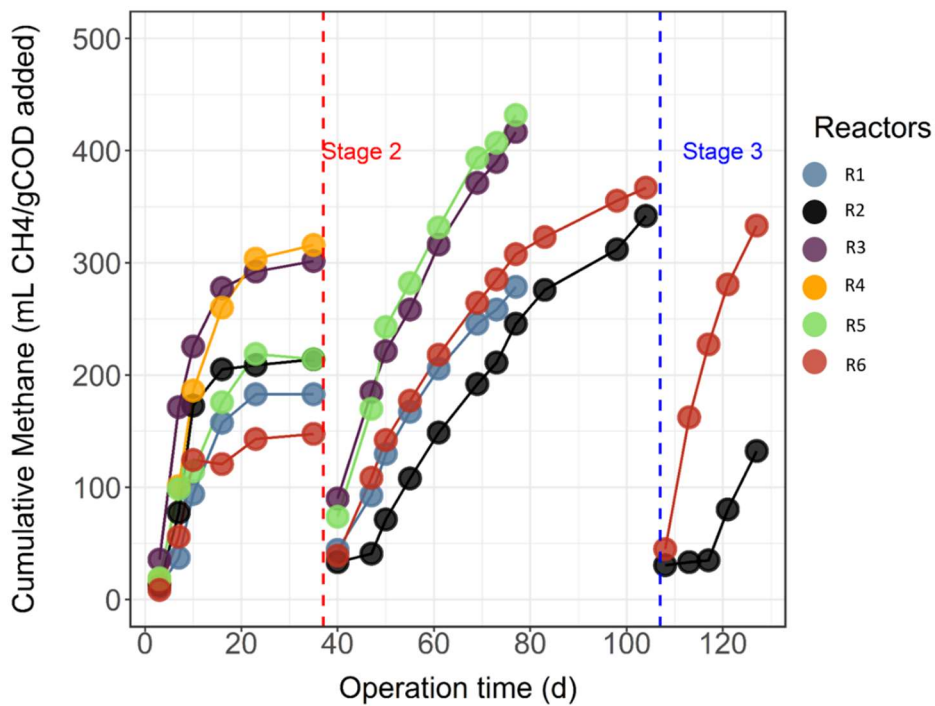


Figure 4.15: Cumulative methane yields from Carbohydrate-based reactors

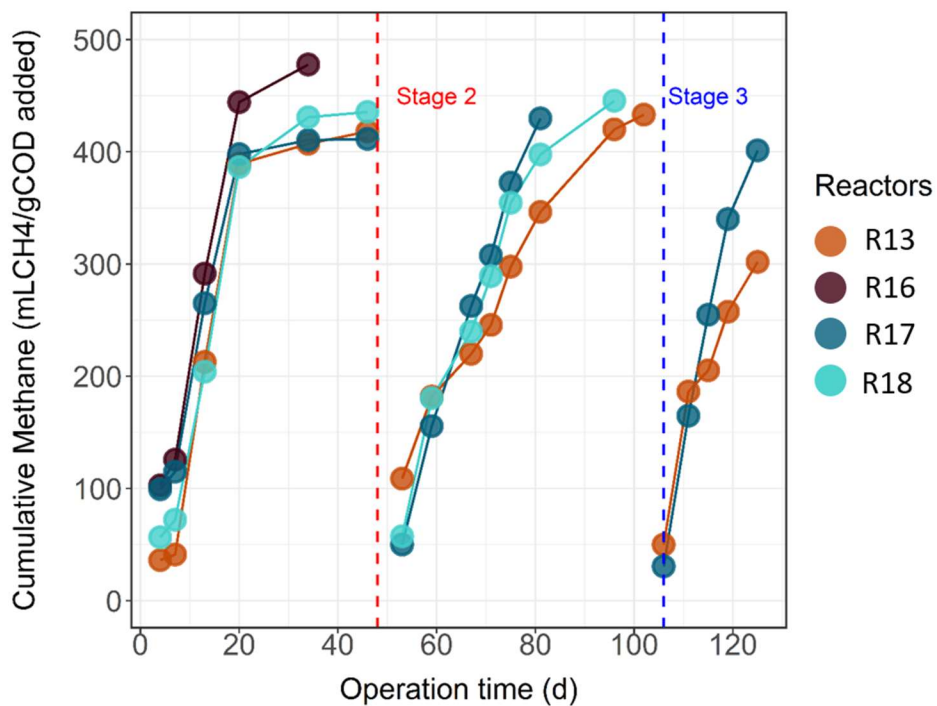


Figure 4.16: Cumulative methane yields from Lipid-based reactors

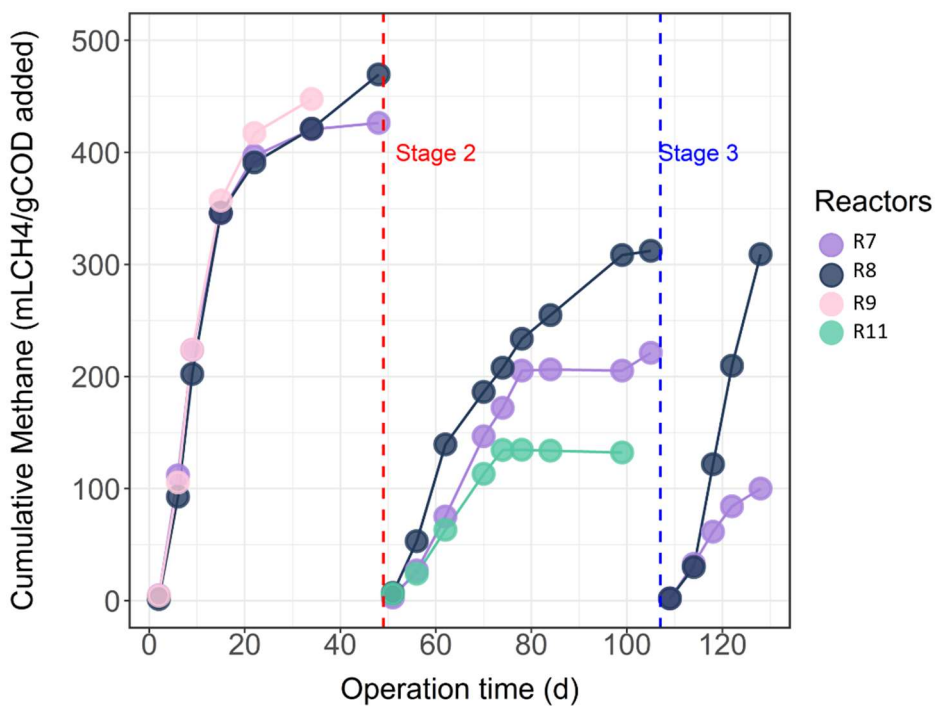


Figure 4.17: Cumulative methane yields from Protein-based reactors

#### 4.4.2 Ammonia Data

By Stage 3, reactors R7, R8 and R17 were above the ammonia threshold stated by McCarty (1964). The ammonia in the remaining reactors increased after loading more protein waste at the beginning of Stage 3 but remained below the threshold.

Table 4.7: Ammonia Concentration in Stage 3

Mixture Point	Substrate	Reactor Code	Start of Stage 3			End of Stage 3			% Change in COD
			(mg NH <sub>3</sub> - N/L)	(g COD/L)	COD/NH <sub>3</sub>	(mg NH <sub>3</sub> - N/L)	(g COD/L)	COD/NH <sub>3</sub>	
A-> E-> G	FVW + FOG + MW	R2	2640 (7.93)	7.66	2.9	2900 (7.9)	6.69	2.3	-12.7
A-> D-> G	FVW + FOG + MW	R6	1200 (7.70)	7.76	6.5	1440 (7.71)	6.11	4.2	-21.3
C-> F-> G	FVW + FOG + MW	R7	5360(8.15)	12.02	2.2	5730 (8.18)	10.62	1.9	-11.6
C-> E-> G	FVW + FOG + MW	R8	6300 (8.19)	15.51	2.5	6340 (8.16)	12.57	2.0	-19.0
B-> D-> G	FVW + FOG + MW	R13	1500 (7.76)	9.33	6.2	1520 (7.78)	7.42	4.9	-20.5
B-> D-> G	FVW + FOG + MW	R17	2850 (7.88)	11.66	4.0	3280 (8.07)	11.3	3.6	-3.1

#### 4.4.3 Stage 3 Discussion

The peak production rates (Figure 4.13) were lower than in Stage 2. There was also a noticeable lag in peak production rates from the protein-based reactors. During Stage 1 and 2, the protein reactors reached peak production rates very early after loading, while the peak took place after the lipid and carbohydrate reactors peaked. The rates in protein reactors are similar to Stage 2, while lipid and carbohydrate-based decreased.

The cumulative yields across all the reactors decreased when introduced to the new substrate type. The yields of the carbohydrate-based and lipid-based seem to decrease the most, while the protein reactors did not experience as much of a change between Stage 2 and Stage 3. The reactors also have low COD/NH<sub>3</sub> ratios at the start of Stage 3, explaining the lower yields than Stages 1 and 2.

## 4.5: Statistical Analysis Results and Discussion

NC State Statistics graduate students were consulted to provide an experimental bioreactor design that included data collection at different mixture points. The experimental design included a statistical analysis of the methane data in determining which substrate mixtures produced the most methane. The analysis consists of running a Scheffé model with the cumulative methane data at each stage. These results provide insight into the optimal substrate mixture for methane production and estimate methane levels for all mixtures in the design space of the simplex centroid model.

Before using the Scheffé models, an Analysis of Variance (ANOVA) was run to verify if the experiment results were significantly different (i.e., reject the null hypothesis). The null hypothesis of this experiment is that various mixtures of substrates do not impact methane yield from anaerobic digesters. The dataset used was the cumulative methane yields at the end of each stage for each reactor (mL CH<sub>4</sub>/ COD<sub>added</sub>). Data from reactors that were leaking data were not included in the statistical analysis. The raw data can be found in the Appendix. A one-way ANOVA test was run in coding language R, analyzing the cumulative methane yields at different ratios. The results of the ANOVA test showed the experimental results as significantly different (F-value 3.237, p-value 0.0171). The Scheffe model was then applied to the different stages. The Scheffé models were run in R using the “mixep” package designed to analyze mixture experiment data.

### 4.5.1 Stage 1: Scheffé Linear Model

At stage one, there is no substrate interaction yet. A Scheffé linear model best analyzes the data from Stage 1 using the following equation:

$$y = \beta_1 x_1 + \beta_2 x_2 + \beta_3 x_3 \text{ (Eq. 4.1)}$$

This model estimates methane production ( $y$ ) from different ratios of substrates. The independent variables  $x_1, x_2, x_3$  represent the proportions of carbohydrate, lipid, and protein waste in a mixture, respectively, and  $\beta_1, \beta_2, \beta_3$  are the parameter estimates for the carbohydrate, lipid and protein terms. The Scheffé model for this data set was plotted over the ternary plot previously introduced (Figure 4.18). This plot shows mixture point B to have produced the most methane per gram of COD, which is 100% FOG-loaded reactors.

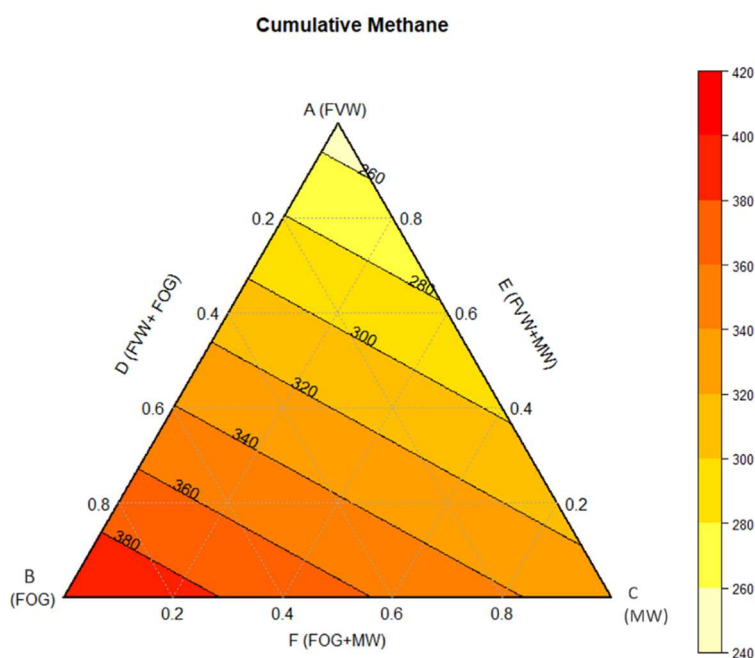


Figure 4.18: Contour Plot of Scheffé Linear Model Response Surface of Stage 1 Cumulative Methane Yield Data

This run found all three substrate types to be significant, therefore all having a different significant impact on the production of methane. The coefficients estimated by the model are all positive values, the largest coefficient being lipid waste. This suggests if a plant is interested in only utilizing one substrate type to maximize gas production, using high lipid substrate would be

the best option. Lipids have the highest methane potential of the three substrate types, so these results agree with past experiments. Although, the  $R^2$  value of this test was 0.2, which is low and implies this model is not a good fit for this data.

Table 4.8: Results from the Scheffé linear model

Substrate	Parameter Estimate	Significant (Y/N)
X1 (FVW)	250	Y
X2( FOG)	400	Y
X3 (MW)	328	Y

#### 4.5.2 Scheffé Quadratic Model for Stage 2 Results

For Stage 2, the Scheffé model is modified to be a quadratic model as now there is an interaction between substrate types. The fitted polynomial is adjusted to accommodate a nonlinear response surface.

$$y = \beta_1x_1 + \beta_2x_2 + \beta_3x_3 + \beta_{12}x_1x_2 + \beta_{23}x_2x_3 + \beta_{13}x_1x_3$$

The response variable ( $y$ ) and  $x_1, x_2, x_3, \beta_1, \beta_2, \beta_3$  represent the same terms as denoted in Equation 4.1 where  $x_1, x_2, x_3$  are the proportions of the substrate in a mixture and  $\beta_1, \beta_2, \beta_3$  are the parameter estimates (carbohydrates, lipids, and protein). The added terms  $\beta_{12}, \beta_{23}, \beta_{13}$  represent the coefficients for the interaction effects between each pair. All of the terms in the equation proved statistically significant, except for “ $\beta_{13}x_1x_3$ ”. This represents the interaction between protein and carbohydrate mixture. The model suggests this mixture is not statistically significant and does not significantly impact methane production. Figure 4.19 displays these results in the ternary plot. The most optimal mixtures indicated by this plot are the FOG and carbohydrate mixture. The negative coefficient (Table 4.9) of the mix between lipid and protein implies

increasing the mixture load will decrease methane production. This was observed in the plots prior, that the introduction of lipid to protein-based decreased the methane yield, as well as introducing protein to lipid-based. The cumulative production increases moving from A (100% FVW) to D (50/50 FOG + FVW) on the ternary plot, suggesting the introduction of FOG improved cumulative methane production from carbohydrate-based reactors, which is shown in the positive coefficient found for this relationship (x1:x2). An increase in cumulative production is observed from mixture point B (100% FOG) when moving towards mixture point D (50/50 FOG + FVW). This mutualistic relationship promotes FOG and FVW as good candidates for co-substrates. It also suggests that the pre-existing communities in A (100% FVW) and B (100% FOG) can adapt to new substrates. The ability of 100% FVW and 100% FOG reactors to adapt well to the introduction of each other in the reactors at mixture point D could be hypothesized by the shared microbial communities that hydrolyze carbohydrates and lipids (Pramanik et al., 2019). The protein reactors yield decreases when moving away from mixture point C (100% MW), defined by the negative coefficients found for protein interactions. This supports earlier suggestions that the pre-existing communities in protein-based reactors could not adjust to the new substrate type. The biogas production increases from A (100% FVW) to E (50/50 FVW + MW), but this interaction was found not significant. Therefore, plants could use MW as a substrate and not expect a significant difference. The  $R^2$  value for this model is 0.4, which is improving from the first model fit.

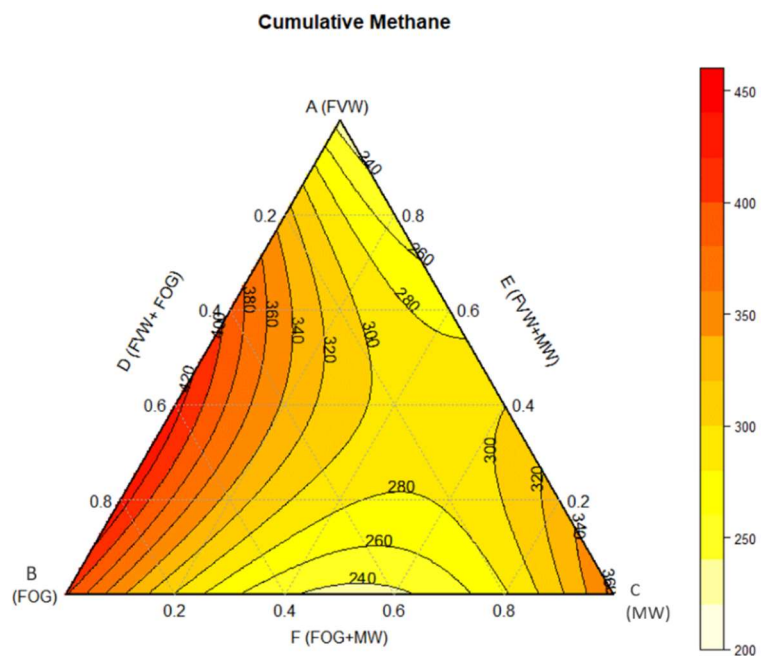


Figure 4.19: Contour Plot of Scheffé Quadratic Model Response Surface of Stage 2 Cumulative Methane Yield Data

Table 4.9: Scheffé Result from Quadratic Model

Substrate	Coefficient	Significance (Y/N)
X1	230	Y
X2	401	Y
X3	366	Y
X1:X2	390	Y
X1:X3	-57	N
X2:X3	-500	Y

#### 4.5.3 Scheffé Special Cubic Model: Stage 3 Methane Data

The last stage is the complete analysis of all the cumulative data points. The final stage of the experiment was loading reactors to mixture point G (equal parts). The Scheffe model now needs to be adjusted to include the interaction between the three substrate types, becoming a special cubic model to accommodate this interaction:

$$y = \beta_1x_1 + \beta_2x_2 + \beta_3x_3 + \beta_{12}x_1x_2 + \beta_{23}x_2x_3 + \beta_{13}x_1x_3 + \beta_{123}x_1x_2x_3$$

While  $y, \beta_1, \beta_2, \beta_3, \beta_{12}, \beta_{23}, \beta_{13}, x_1, x_2, x_3$  remain the same as in Eq. 4.2, the newly introduced parameter ( $\beta_{123}$ ) is the coefficient of interaction between all three substrate types. From this run, the loading of the three substrate types, mixture point G, was found not to be statistically significant. Combining the three food waste types did not significantly impact methane generation. Thus mixing the three types of food waste does not optimize methane production. The same conclusion was drawn for mixture points E (MW + FVW) and F (MW+ FOG). These interactions were insignificant, indicating that these mixtures do not optimize methane production. Mixture point D (FOG + FVW) is the only significant parameter of the substrate mixtures. The other significant parameters, A, B, and C, are 100% of one type. These results emphasize the importance of microbial communities specific to substrate types and the different range of abilities to transform food waste into methane.

Table 4.10: Scheffé model results for stage 3 data

<b>Substrate</b>	<b>Coefficient</b>	<b>Significance</b>
X1	227	Y
X2	397	Y
X3	362	Y
X1:X2	491	Y
X1:X3	72	N
X2:X3	-420	N
X1:X2:X3	-1000	N

These results are presented in the contour plot in Figure 4.20. As observed in the plot, the cumulative methane yield decreases when moving to mixture point G from any vertex or mixture point. While the production declines while moving towards G, this mixture point was found not significant by the Scheffé test. Previous conclusions from the Stage 2 results are in accordance with these results, in that mixture point D is the most optimal for cumulative methane yield.

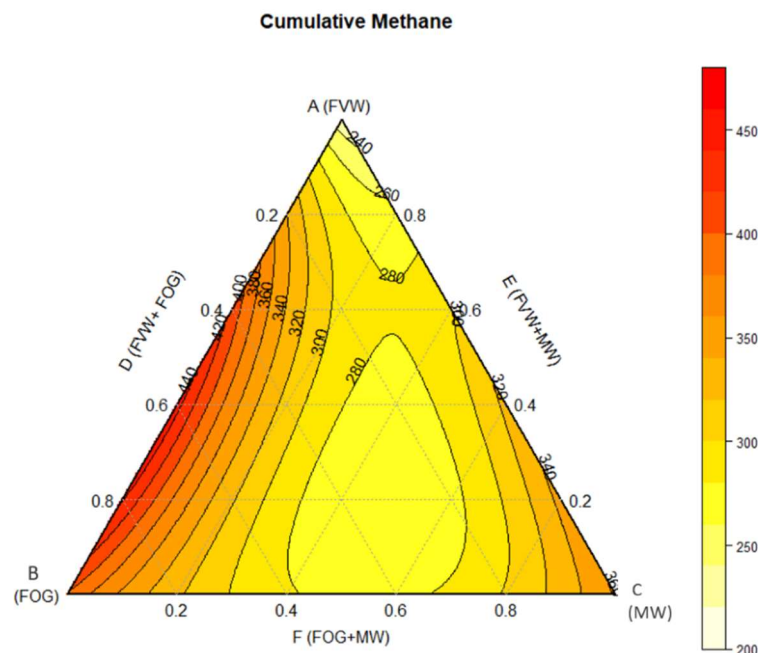


Figure 4.20: Contour Plot of Scheffé Special Cubic Model Response Surface

It is essential to note the limitations of using these models to analyze the influence of various substrate types on methane production. Scheffe models are typically conservative methods and have the lowest statistical power. However, this method was chosen to compare all possible simple and complex pairs of data points in the data set. Additionally, this model assumes that the substrate type is the only influence on biogas production from anaerobic co-digestion. Multiple other parameters that influence biogas production should be included, specifically the microbial community's diversity, richness, and evenness, temperatures, pH values, and C/N ratios, to create a more comprehensive model to estimate biogas production.

## CHAPTER 5: Conclusions

The objective of this research was to understand the influence of various food waste types and mixtures on methane production and microbial communities to help develop operational procedures for full-scale adaptation. From the process performance data and the statistical analysis, it is evident that the optimal mixture of food waste for cumulative methane production is lipids and carbohydrates. These reactors produced the highest methane yield and had the highest coefficient from the statistical analysis. Lipid waste had the highest cumulative production of the reactors loaded with one type of food waste. 100% protein waste also had high cumulative yields, but results from the further stages suggest that the communities in protein-fed reactors are not as resilient to substrate changes as the lipid and carbohydrate-fed systems.

The peak production rates also provided insight into the start-up time of reactors. Carbohydrates and protein were the fastest to achieve peak production rates in Stage 1. Protein-based reactors took longer to hit peak production rates in Stage 3 when the reactors were loaded with all three substrate types. While protein is not the suggested first substrate to build the microbial community in a digester, it increases methane production when loaded into previously fed carbohydrate-based reactors.

The mixture points found statistically significant toward cumulative methane production were D (FOG + FVW), A (FVW), B (FOG), and C (MW). The remaining mixture points E (FVW + MW), F (MW and FOG), and G (FVW + FOG + MW) were found not to be statistically significant, therefore not significantly impacting methane production. Thus data from mixture points A, B, C and D can be used in optimizing methane production, but the other mixture points were not significantly different. Plants can expect an insignificant change in biogas production

when loading at these other mixture points. Of course, the impact of these mixture points will depend on what was previously loaded into the reactor.

Recommendations for full-scale operations would include to avoid starting a digester with protein substrate as the microbial communities that develop from protein as a substrate are not as robust to substrate changes compared to reactors started with carbohydrate or lipid waste. The plant can expect an increase in biogas production if loading a mixture of FVW and FOG to a reactor previously loaded with either of these substrates. The statistical analysis finds that the other mixtures are insignificant to cumulative methane production. However, if plants receive a large load of MW to feed reactors, they can expect high ammonia accumulation and low C/N ratios that may impact biogas production. While full-scale operations likely do not have much control over the substrate they receive, they do have control over how much they are loading into a system and may have options to mix substrates for better performance. Understanding these changes can help them prepare to address these parameters.

To date, there is little insight into the shifts in microbial communities when introduced different mixtures of substrate types. This is critical information needed for full-scale adaptation so plants can maintain optimal biogas conditions and understand how the substrate mixtures will impact essential parameters such as C/N ratios and ammonia concentrations, resulting in a shift in the microbial community. Microbial community analysis will occur in the near future to answer these questions.

Additional future work is to create a model that can accurately predict cumulative methane production from different proportions of substrate types. The models used in this study will provide an estimate based on the data from different experiment stages. Still, the model could be developed to include other essential parameters such as microbial communities, C/N

ratios, temperature, and pH. Anaerobic co-digestion is a complex system with many influential factors that can change biogas production. Including these parameters to develop a comprehensive model of AcD would benefit plants in estimating the expected methane from their digesters from different substrate types, therefore allowing more control over the AcD performance.

## REFERENCES

- Angelidaki, I., & Ahring, B. K. (1994). Anaerobic thermophilic digestion of manure at different ammonia loads: Effect of temperature. *Water Research*, *28*(3), 727–731.  
[https://doi.org/10.1016/0043-1354\(94\)90153-8](https://doi.org/10.1016/0043-1354(94)90153-8)
- Bardi, M. J., & Aminirad, H. (2020). Synergistic effects of co-trace elements on anaerobic co-digestion of food waste and sewage sludge at high organic load. *Environmental Science and Pollution Research*, *27*(15), 18129–18144. <https://doi.org/10.1007/s11356-020-08252-y>
- Bi, S., Hong, X., Yang, H., Yu, X., Fang, S., Bai, Y., Liu, J., Gao, Y., Yan, L., Wang, W., & Wang, Y. (2020). Effect of hydraulic retention time on anaerobic co-digestion of cattle manure and food waste. *Renewable Energy*, *150*, 213–220.  
<https://doi.org/10.1016/j.renene.2019.12.091>
- Bolzonella, D., Battistoni, P., Susini, C., & Cecchi, F. (2006). Anaerobic codigestion of waste activated sludge and OFMSW: The experiences of Viareggio and Treviso plants (Italy). *Water Science and Technology*, *53*(8), 203–211. <https://doi.org/10.2166/wst.2006.251>
- Chen, Ye, Cheng, J. J., & Creamer, K. S. (2008). Inhibition of anaerobic digestion process: A review. *Bioresource Technology*, *99*(10), 4044–4064.  
<https://doi.org/10.1016/j.biortech.2007.01.057>
- Chen, Yunmin, Xu, W., Zhan, L., Ke, H., Hu, J., Li, H., Ma, P., & Li, J. (2021). Geoenvironmental Issues in High-Food-Waste-Content Municipal Solid Waste Landfills. *Journal of the Indian Institute of Science*, *101*(4), 603–623. <https://doi.org/10.1007/s41745-021-00233-5>
- Dalke, R., Demro, D., Khalid, Y., Wu, H., & Urgun-Demirtas, M. (2021). Current status of anaerobic digestion of food waste in the United States. *Renewable and Sustainable Energy*

- Reviews*, 151(September 2020), 111554. <https://doi.org/10.1016/j.rser.2021.111554>
- De Clercq, D., Wen, Z., Gottfried, O., Schmidt, F., & Fei, F. (2017). A review of global strategies promoting the conversion of food waste to bioenergy via anaerobic digestion. *Renewable and Sustainable Energy Reviews*, 79(May), 204–221. <https://doi.org/10.1016/j.rser.2017.05.047>
- Deepanraj, B., Sivasubramanian, V., & Jayaraj, S. (2014). Biogas generation through anaerobic digestion process-an overview. *Research Journal of Chemistry and Environment*, 18(5), 80–94.
- González-Fernández, C., & García-Encina, P. A. (2009). Impact of substrate to inoculum ratio in anaerobic digestion of swine slurry. In *Biomass and Bioenergy* (Vol. 33, Issue 8, pp. 1065–1069). <https://doi.org/10.1016/j.biombioe.2009.03.008>
- Hagos, K., Zong, J., Li, D., Liu, C., & Lu, X. (2017). Anaerobic co-digestion process for biogas production: Progress, challenges and perspectives. *Renewable and Sustainable Energy Reviews*, 76(November 2016), 1485–1496. <https://doi.org/10.1016/j.rser.2016.11.184>
- Karki, R., Chuenchart, W., Surendra, K. C., Shrestha, S., Raskin, L., Sung, S., Hashimoto, A., & Kumar Khanal, S. (2021). Anaerobic co-digestion: Current status and perspectives. *Bioresource Technology*, 330(January), 125001. <https://doi.org/10.1016/j.biortech.2021.125001>
- Kaur, G., Luo, L., Chen, G., & Wong, J. W. C. (2019). Integrated food waste and sewage treatment – A better approach than conventional food waste-sludge co-digestion for higher energy recovery via anaerobic digestion. *Bioresource Technology*, 289(June), 121698. <https://doi.org/10.1016/j.biortech.2019.121698>
- Kearns, J. (2013). Synthetic chemical water contaminants: an often overlooked challenge in

- international sustainable community development. *ECHO Asia Notes*, 17.  
[http://c.ymcdn.com/sites/members.echocommunity.org/resource/collection/0ADF35ED-72B3-44AA-92B5-D50F9B4A741D/AN\\_17.pdf](http://c.ymcdn.com/sites/members.echocommunity.org/resource/collection/0ADF35ED-72B3-44AA-92B5-D50F9B4A741D/AN_17.pdf)
- Kim, H. W., Han, S. K., & Shin, H. S. (2003). The optimisation of food waste addition as a co-substrate in anaerobic digestion of sewage sludge. *Waste Management and Research*, 21(6), 515–526. <https://doi.org/10.1177/0734242X0302100604>
- Kim, M. S., Kim, D. H., & Yun, Y. M. (2017). Effect of operation temperature on anaerobic digestion of food waste: Performance and microbial analysis. In *Fuel* (Vol. 209, pp. 598–605). <https://doi.org/10.1016/j.fuel.2017.08.033>
- Levis, J. W., & Barlaz, M. A. (2011). What is the most environmentally beneficial way to treat commercial food waste? *Environmental Science and Technology*, 45(17), 7438–7444. <https://doi.org/10.1021/es103556m>
- Li, L., He, Q., Ma, Y., Wang, X., & Peng, X. (2015). Dynamics of microbial community in a mesophilic anaerobic digester treating food waste: Relationship between community structure and process stability. *Bioresource Technology*, 189, 113–120. <https://doi.org/10.1016/j.biortech.2015.04.015>
- Li, L., Peng, X., Wang, X., & Wu, D. (2018). Anaerobic digestion of food waste: A review focusing on process stability. *Bioresource Technology*, 248(174), 20–28. <https://doi.org/10.1016/j.biortech.2017.07.012>
- Liao, X., Zhu, S., Zhong, D., Zhu, J., & Liao, L. (2014). Anaerobic co-digestion of food waste and landfill leachate in single-phase batch reactors. *Waste Management*, 34(11), 2278–2284. <https://doi.org/10.1016/j.wasman.2014.06.014>
- Lin, Q., De Vrieze, J., He, G., Li, X., & Li, J. (2016). Temperature regulates methane production

through the function centralization of microbial community in anaerobic digestion.

*Bioresource Technology*, 216, 150–158. <https://doi.org/10.1016/j.biortech.2016.05.046>

Lv, Y., Chang, N., Li, Y. Y., & Liu, J. (2021a). Anaerobic co-digestion of food waste with municipal solid waste leachate: A review and prospective application with more benefits. *Resources, Conservation and Recycling*, 174(March), 105832.

<https://doi.org/10.1016/j.resconrec.2021.105832>

Lv, Y., Chang, N., Li, Y. Y., & Liu, J. (2021b). Anaerobic co-digestion of food waste with municipal solid waste leachate: A review and prospective application with more benefits. *Resources, Conservation and Recycling*, 174(July), 105832.

<https://doi.org/10.1016/j.resconrec.2021.105832>

Mata-Alvarez, J., Dosta, J., Romero-Güiza, M. S., Fonoll, X., Peces, M., & Astals, S. (2014). A critical review on anaerobic co-digestion achievements between 2010 and 2013. *Renewable and Sustainable Energy Reviews*, 36, 412–427. <https://doi.org/10.1016/j.rser.2014.04.039>

Mehariya, S., Patel, A. K., Obulisamy, P. K., Punniyakotti, E., & Wong, J. W. C. (2018). Co-digestion of food waste and sewage sludge for methane production: Current status and perspective. *Bioresource Technology*, 265(April), 519–531.

<https://doi.org/10.1016/j.biortech.2018.04.030>

Nghiem, L. D., Koch, K., Bolzonella, D., & Drewes, J. E. (2017). Full scale co-digestion of wastewater sludge and food waste: Bottlenecks and possibilities. *Renewable and Sustainable Energy Reviews*, 72(November 2016), 354–362.

<https://doi.org/10.1016/j.rser.2017.01.062>

Owen, P. (1986). *Fundamentals of anaerobic digestion of wastewater sludges*.

Papargyropoulou, E., Lozano, R., K. Steinberger, J., Wright, N., & Ujang, Z. Bin. (2014). The

- food waste hierarchy as a framework for the management of food surplus and food waste. In *Journal of Cleaner Production* (Vol. 76, pp. 106–115).  
<https://doi.org/10.1016/j.jclepro.2014.04.020>
- Parkin, G. F., & Owen, W. F. (1986). Fundamentals of Anaerobic Digestion of Wastewater Sludges. *Journal of Environmental Engineering*, 112(5), 867–920.  
[https://doi.org/10.1061/\(asce\)0733-9372\(1986\)112:5\(867\)](https://doi.org/10.1061/(asce)0733-9372(1986)112:5(867))
- Perry L. McCarty. (1964). Anaerobic Waste Treatment Fundamentals. In *Public Works* (Vol. 98, Issue 1, pp. 9–12). <http://extension.psu.edu/natural-resources/energy/waste-to-energy/resources/biogas/links/the-anaerobic-digestion-process/mccarty-anaerobic-overview.pdf>
- Pramanik, S. K., Suja, F. B., Zain, S. M., & Pramanik, B. K. (2019). The anaerobic digestion process of biogas production from food waste: Prospects and constraints. *Bioresource Technology Reports*, 8(August), 100310. <https://doi.org/10.1016/j.biteb.2019.100310>
- Qiagen. (2018). *DNeasy® PowerSoil® Pro Kit*. May, 9–10.
- Rajagopal, R., Massé, D. I., & Singh, G. (2013). A critical review on inhibition of anaerobic digestion process by excess ammonia. *Bioresource Technology*, 143, 632–641.  
<https://doi.org/10.1016/j.biortech.2013.06.030>
- Sanders, W. T. M., Geerink, M., Zeeman, G., & Lettinga, G. (2000). Anaerobic hydrolysis kinetics of particulate substrates. *Water Science and Technology*, 41(3), 17–24.  
<https://doi.org/10.2166/wst.2000.0051>
- Shahbaz, M., Ammar, M., Zou, D., Korai, R. M., & Li, X. J. (2019). An Insight into the Anaerobic Co-digestion of Municipal Solid Waste and Food Waste: Influence of Co-substrate Mixture Ratio and Substrate to Inoculum Ratio on Biogas Production. *Applied*

*Biochemistry and Biotechnology*, 187(4), 1356–1370. <https://doi.org/10.1007/s12010-018-2891-3>

Shen, Y., Linville, J. L., Urgan-Demirtas, M., Mintz, M. M., & Snyder, S. W. (2015). An overview of biogas production and utilization at full-scale wastewater treatment plants (WWTPs) in the United States: Challenges and opportunities towards energy-neutral WWTPs. *Renewable and Sustainable Energy Reviews*, 50, 346–362. <https://doi.org/10.1016/j.rser.2015.04.129>

Shi, X., Lin, J., Zuo, J., Li, P., Li, X., & Guo, X. (2017). Effects of free ammonia on volatile fatty acid accumulation and process performance in the anaerobic digestion of two typical bio-wastes. *Journal of Environmental Sciences (China)*, 55, 49–57. <https://doi.org/10.1016/j.jes.2016.07.006>

Sillas-Moreno, M. V., Senés-Guerrero, C., Pacheco, A., & Montesinos-Castellanos, A. (2019). Methane potential and metagenomics of wastewater sludge and a methane-producing landfill solid sample as microbial inocula for anaerobic digestion of food waste. *Journal of Chemical Technology and Biotechnology*, 94(4), 1123–1133. <https://doi.org/10.1002/jctb.5859>

Slorach, P. C., Jeswani, H. K., Cuéllar-Franca, R., & Azapagic, A. (2019). Environmental sustainability of anaerobic digestion of household food waste. In *Journal of Environmental Management* (Vol. 236, pp. 798–814). <https://doi.org/10.1016/j.jenvman.2019.02.001>

Speece, R. E. (1983). Anaerobic biotechnology for industrial wastewater treatment. *Environmental Science and Technology*, 17(9), 416A-427A. <https://doi.org/10.1021/es00115a001>

Staley, B. F., Saikaly, P. E., de los Reyes, F. L., & Barlaz, M. A. (2011). Critical evaluation of

solid waste sample processing for DNA-based microbial community analysis.

*Biodegradation*, 22(1), 189–204. <https://doi.org/10.1007/s10532-010-9387-3>

Syaichurrozi, I., Budiyo, & Sumardiono, S. (2013). Predicting kinetic model of biogas production and biodegradability organic materials: Biogas production from vinasse at variation of COD/N ratio. In *Bioresource Technology* (Vol. 149, pp. 390–397).

<https://doi.org/10.1016/j.biortech.2013.09.088>

Tyagi, V. K., Fdez-Güelfo, L. A., Zhou, Y., Álvarez-Gallego, C. J., Garcia, L. I. R., & Ng, W. J. (2018). Anaerobic co-digestion of organic fraction of municipal solid waste (OFMSW): Progress and challenges. In *Renewable and Sustainable Energy Reviews* (Vol. 93, pp. 380–399). Elsevier Ltd. <https://doi.org/10.1016/j.rser.2018.05.051>

USDA. “Food Availability (per Capita) Data System.” *USDA ERS - Food Availability (Per Capita) Data System*, 2021, <https://www.ers.usda.gov/data-products/food-availability-per-capita-data-system/>.

Wagner, A. O., Lins, P., Malin, C., Reitschuler, C., & Illmer, P. (2013). Impact of protein-, lipid- and cellulose-containing complex substrates on biogas production and microbial communities in batch experiments. *Science of the Total Environment*, 458–460, 256–266.

<https://doi.org/10.1016/j.scitotenv.2013.04.034>

Wang, L. (2018). *Influencing the Anaerobic Microbiome through Substrate Selection and Overloading Stresses to Achieve High-Performance Co-Digestion of Grease Interceptor Waste*.

Wang, P., Wang, H., Qiu, Y., Ren, L., & Jiang, B. (2018). Microbial characteristics in anaerobic digestion process of food waste for methane production—A review. *Bioresource Technology*, 248, 29–36. <https://doi.org/10.1016/j.biortech.2017.06.152>

Wang, Z., Jiang, Y., Wang, S., Zhang, Y., Hu, Y., Hu, Z. hu, Wu, G., & Zhan, X. (2020). Impact

of total solids content on anaerobic co-digestion of pig manure and food waste: Insights into shifting of the methanogenic pathway. *Waste Management*, 114, 96–106.

<https://doi.org/10.1016/j.wasman.2020.06.048>

Westerholm, M., Moestedt, J., & Schnürer, A. (2016). Biogas production through syntrophic acetate oxidation and deliberate operating strategies for improved digester performance.

*Applied Energy*, 179, 124–135. <https://doi.org/10.1016/J.APENERGY.2016.06.061>

Wood, A., Dulaney, D., & Edikala, A. (n.d.). *Designing a Bioreactor Experiment*. 1–20.

Xu, S., Selvam, A., & Wong, J. W. C. (2014). Optimization of micro-aeration intensity in

acidogenic reactor of a two-phase anaerobic digester treating food waste. *Waste*

*Management*, 34(2), 363–369. <https://doi.org/10.1016/j.wasman.2013.10.038>

Zahan, Z., Georgiou, S., Muster, T. H., & Othman, M. Z. (2018). Semi-continuous anaerobic co-

digestion of chicken litter with agricultural and food wastes: A case study on the effect of carbon/nitrogen ratio, substrates mixing ratio and organic loading. In *Bioresource*

*Technology* (Vol. 270, pp. 245–254). <https://doi.org/10.1016/j.biortech.2018.09.010>

Zhang, C., Xiao, G., Peng, L., Su, H., & Tan, T. (2013). The anaerobic co-digestion of food waste and cattle manure. *Bioresource Technology*, 129, 170–176.

<https://doi.org/10.1016/j.biortech.2012.10.138>

Zhang, H., Liu, G., Xue, L., Zuo, J., Chen, T., Vuppaladadiyam, A., & Duan, H. (2020).

Anaerobic digestion based waste-to-energy technologies can halve the climate impact of China's fast-growing food waste by 2040. *Journal of Cleaner Production*, 277, 123490.

<https://doi.org/10.1016/j.jclepro.2020.123490>

Zhang, Wanli, Wang, X., Xing, W., Li, R., Yang, T., Yao, N., & Lv, D. (2021). Links between synergistic effects and microbial community characteristics of anaerobic co-digestion of

food waste, cattle manure and corn straw. *Bioresource Technology*, 329(March), 124919.

<https://doi.org/10.1016/j.biortech.2021.124919>

Zhang, Wanli, Zhang, L., & Li, A. (2015a). Anaerobic co-digestion of food waste with MSW incineration plant fresh leachate: Process performance and synergistic effects. *Chemical Engineering Journal*, 259, 795–805. <https://doi.org/10.1016/j.cej.2014.08.039>

Zhang, Wanli, Zhang, L., & Li, A. (2015b). The positive effects of waste leachate addition on methane fermentation from food waste in batch trials. *Water Science and Technology*, 72(3), 429–436. <https://doi.org/10.2166/wst.2015.231>

Zhang, Wei, Werner, J. J., Agler, M. T., & Angenent, L. T. (2014). Substrate type drives variation in reactor microbiomes of anaerobic digesters. In *Bioresource Technology* (Vol. 151, pp. 397–401). <https://doi.org/10.1016/j.biortech.2013.10.004>

Zheng, Y., Wang, P., Yang, X., Lin, P., Wang, Y., Cheng, M., & Ren, L. (2021). Process Performance and Microbial Communities in Anaerobic Co-digestion of Sewage Sludge and Food Waste with a Lower Range of Carbon/Nitrogen Ratio. *Bioenergy Research*, 0123456789. <https://doi.org/10.1007/s12155-021-10357-2>

**APPENDICES**

**Appendix A: Ammonia Concentration Measurements**

Test Date	Sample ID	NH3 Reading	Dilution factor	mg/L-N
10/13/2021	R1	5.2	100.00	520
10/13/2021	R2	12.3	100.00	1230
10/13/2021	R3	13.7	100.00	1370
10/13/2021	R4	2.3	100.00	230
10/13/2021	R5	13.9	100.00	1390
10/13/2021	R6	13.7	100.00	1370
10/13/2021	R7	38.7	100.00	3870
10/13/2021	R8	39	100.00	3900
10/13/2021	R9	15.4	100.00	1540
10/13/2021	R10	46.2	100.00	4620
10/13/2021	R11	39.8	100.00	3980
10/13/2021	R12	39	100.00	3900
10/13/2021	R13	11.4	100.00	1140
10/13/2021	R14	3.1	100.00	310
10/13/2021	R15	11.8	100.00	1180
10/13/2021	R16	10.9	100.00	1090
10/13/2021	R17	9.9	100.00	990
10/13/2021	R18	10.9	100.00	1090
10/13/2021	R19	12.8	100.00	1280
10/13/2021	R20	10.9	100.00	1090
10/13/2021	R21	13.5	100.00	1350
11/11/2021	R1	12.4	100.00	1240
11/11/2021	R2	11.1	100.00	1110
11/11/2021	R3	13.2	100.00	1320
11/11/2021	R4	13.3	100.00	1330
11/11/2021	R5	11.4	100.00	1140
11/11/2021	R6	10.8	100.00	1080
11/11/2021	R7	46.3	100.00	4630
11/11/2021	R8	45	100.00	4500
11/11/2021	R9	44	100.00	4400
11/11/2021	R10	5	1000.00	5000
11/11/2021	R11	45.6	100.00	4560
11/11/2021	R12	40.8	100.00	4080
11/11/2021	R13	11	100.00	1100
11/11/2021	R14	10.5	100.00	1050

11/11/2021	R15	10.1	100.00	1010
11/11/2021	R16	10.7	100.00	1070
11/11/2021	R17	11.1	100.00	1110
11/11/2021	R18	10	100.00	1000
11/11/2021	R19	10.2	100.00	1020
11/11/2021	R20	11.8	100.00	1180
11/11/2021	R21	12.8	100.00	1280
11/23/2021	R1	17.9	100.00	1790
11/23/2021	R2	16.8	100.00	1680
11/23/2021	R3	14.6	100.00	1460
11/23/2021	R5	12.1	100.00	1210
11/23/2021	R6	11.2	100.00	1120
11/23/2021	R7	42.6	100.00	4260
11/23/2021	R8	43.8	100.00	4380
11/23/2021	R10	49	100.00	4900
11/23/2021	R11	50.8	100.00	5080
11/23/2021	R13	11.4	100.00	1140
11/23/2021	R15	10.3	100.00	1030
11/23/2021	R17	12.9	100.00	1290
11/23/2021	R18	11.3	100.00	1130
11/23/2021	R19	12.5	100.00	1250
11/23/2021	R20	12.4	100.00	1240
11/23/2021	R21	12.8	100.00	1280
11/30/2021	R1	21	100.00	2100
11/30/2021	R2	18.2	100.00	1820
11/30/2021	R3	15.8	100.00	1580
11/30/2021	R5	12.1	100.00	1210
11/30/2021	R6	11.2	100.00	1120
11/30/2021	R7	4.1	100.00	410
11/30/2021	R8	4.1	100.00	410
11/30/2021	R10	4.8	100.00	480
11/30/2021	R11	4.8	100.00	480
11/30/2021	R13	11.3	100.00	1130
11/30/2021	R15	9.8	100.00	980
11/30/2021	R17	13.7	100.00	1370
11/30/2021	R18	16	100.00	1600
11/30/2021	R19	11.2	100.00	1120
11/30/2021	R20	11.9	100.00	1190
11/30/2021	R21	11.7	100.00	1170
12/8/2021	R1	23	100.00	2300
12/8/2021	R2	21.1	100.00	2110
12/8/2021	R3	16.1	100.00	1610
12/8/2021	R5	12.3	100.00	1230
12/8/2021	R6	12.4	100.00	1240

12/8/2021	R7	5.6	1000.00	5600
12/8/2021	R8	5.1	1000.00	5100
12/8/2021	R10	5.5	1000.00	5500
12/8/2021	R11	5.7	1000.00	5700
12/8/2021	R13	12.4	100.00	1240
12/8/2021	R15	10	100.00	1000
12/8/2021	R17	18.1	100.00	1810
12/8/2021	R18	25	100.00	2500
12/8/2021	R19	12.5	100.00	1250
12/8/2021	R20	11.3	100.00	1130
12/8/2021	R21	12.6	100.00	1260
12/13/2021	R1	23.6	100.00	2360
12/13/2021	R2	22.8	100.00	2280
12/13/2021	R3	16.8	100.00	1680
12/13/2021	R5	11.9	100.00	1190
12/13/2021	R6	12.4	100.00	1240
12/13/2021	R7	5.2	1000.00	5200
12/13/2021	R8	5.6	1000.00	5600
12/13/2021	R10	5.8	1000.00	5800
12/13/2021	R11	6	1000.00	6000
12/13/2021	R13	11.1	100.00	1110
12/13/2021	R15	10.5	100.00	1050
12/13/2021	R17	22.5	100.00	2250
12/13/2021	R18	27.8	100.00	2780
12/13/2021	R19	10.7	100.00	1070
12/13/2021	R20	11.4	100.00	1140
12/13/2021	R21	12.3	100.00	1230
1/5/2022	R2	24.3	100.00	2430
1/5/2022	R6	12.4	100.00	1240
1/5/2022	R7	5.1	1000.00	5100
1/5/2022	R8	6	1000.00	6000
1/5/2022	R10	6.7	1000.00	6700
1/5/2022	R11	5.8	1000.00	5800
1/5/2022	R13	11.3	100.00	1130
1/5/2022	R15	15.7	100.00	1570
1/5/2022	R17	27.3	100.00	2730
1/5/2022	R18	29.4	100.00	2940
1/21/2022	R2	26.4	100.00	2640
1/21/2022	R6	12	100.00	1200
1/21/2022	R7	1.5	1000.00	1500
1/21/2022	R8	6.3	1000.00	6300
1/21/2022	R13	53.6	100.00	5360
1/21/2022	R17	28.5	100.00	2850
1/25/2022	R2	28.3	100.00	2830

1/25/2022	R6	13.2	100.00	1320
1/25/2022	R7	5.4	1000.00	5400
1/25/2022	R8	5.6	1000.00	5600
1/25/2022	R13	13.2	100.00	1320
1/25/2022	R17	29.8	100.00	2980
1/31/2022	R2	29	100.00	2900
1/31/2022	R6	14.4	100.00	1440
1/31/2022	R7	57.3	100.00	5730
1/31/2022	R8	63.4	100.00	6340
1/31/2022	R13	15.2	100.00	1520
1/31/2022	R17	32.8	100.00	3280

### Appendix B: Cumulative Methane Data

Days Since Start	mLCH <sub>4</sub> gCOD	Reactors
3	11.1	R1_S1
7	37.1	R1_S1
10	94.1	R1_S1
16	157.5	R1_S1
23	182.9	R1_S1
35	183.0	R1_S1
42	44.3	R1_S2
49	92.7	R1_S2
52	129.8	R1_S2
57	167.2	R1_S2
63	205.8	R1_S2
71	245.8	R1_S2
75	258.4	R1_S2
79	278.7	R1_S2
3	12.5	R2_S1
7	77.5	R2_S1
10	172.8	R2_S1
16	205.1	R2_S1
23	208.8	R2_S1
35	214.1	R2_S1
42	33.2	R2_S2
49	40.9	R2_S2
52	71.3	R2_S2
57	107.9	R2_S2
63	148.8	R2_S2
71	192.0	R2_S2
75	211.2	R2_S2
79	245.7	R2_S2
85	275.9	R2_S2
100	312.0	R2_S2
106	341.9	R2_S2
114	30.6	R2_S3
119	33.2	R2_S3
123	34.9	R2_S3
127	80.2	R2_S3

133	132.3	R2_S3
3	35.5	R3_S1
7	171.4	R3_S1
10	225.5	R3_S1
16	277.7	R3_S1
23	292.3	R3_S1
35	301.6	R3_S1
42	90.1	R3_S2
49	185.0	R3_S2
52	221.3	R3_S2
57	258.4	R3_S2
63	316.3	R3_S2
71	371.4	R3_S2
75	389.9	R3_S2
79	416.7	R3_S2
3	17.8	R4_S1
7	101.1	R4_S1
10	186.2	R4_S1
16	260.1	R4_S1
23	303.7	R4_S1
35	316.0	R4_S1
3	19.0	R5_S1
7	98.5	R5_S1
10	114.4	R5_S1
16	175.8	R5_S1
23	218.9	R5_S1
35	214.1	R5_S1
42	73.7	R5_S2
49	170.0	R5_S2
52	242.8	R5_S2
57	282.0	R5_S2
63	331.7	R5_S2
71	393.4	R5_S2
75	407.0	R5_S2
79	431.8	R5_S2
3	8.5	R6_S1
7	55.8	R6_S1
10	124.2	R6_S1
16	120.7	R6_S1
23	143.1	R6_S1

35	147.6	R6_S1
42	39.0	R6_S2
49	108.5	R6_S2
52	142.1	R6_S2
57	177.1	R6_S2
63	218.1	R6_S2
71	264.4	R6_S2
75	285.3	R6_S2
79	307.7	R6_S2
85	323.1	R6_S2
100	355.3	R6_S2
106	366.9	R6_S2
114	44.8	R6_S3
119	162.3	R6_S3
123	227.2	R6_S3
127	280.7	R6_S3
133	333.2	R6_S3
2	4.8	R7_S1
6	111.7	R7_S1
9	223.6	R7_S1
15	345.5	R7_S1
22	396.9	R7_S1
34	420.6	R7_S1
48	426.3	R7_S1
51	2.8	R7_S2
56	26.9	R7_S2
62	75.0	R7_S2
70	146.6	R7_S2
74	172.0	R7_S2
78	205.2	R7_S2
84	206.3	R7_S2
99	205.2	R7_S2
105	221.1	R7_S2
113	1.9	R7_S3
118	32.8	R7_S3
122	61.5	R7_S3
126	148.0	R7_S3
132	248.0	R7_S3
2	1.3	R8_S1
6	92.7	R8_S1

9	202.2	R8_S1
15	346.2	R8_S1
22	391.0	R8_S1
34	421.2	R8_S1
48	469.5	R8_S1
51	6.8	R8_S2
56	53.0	R8_S2
62	139.4	R8_S2
70	186.2	R8_S2
74	207.8	R8_S2
78	233.7	R8_S2
84	254.8	R8_S2
99	308.4	R8_S2
105	312.1	R8_S2
113	2.0	R8_S3
118	29.9	R8_S3
122	121.7	R8_S3
126	209.7	R8_S3
132	309.2	R8_S3
2	4.4	R9_S1
6	105.4	R9_S1
9	224.0	R9_S1
15	357.1	R9_S1
22	417.4	R9_S1
34	447.7	R9_S1
2	2.7	R10_S1
6	76.0	R10_S1
9	176.2	R10_S1
15	311.8	R10_S1
22	356.0	R10_S1
34	386.0	R10_S1
48	407.0	R10_S1
51	2.0	R10_S2
56	3.0	R10_S2
62	50.0	R10_S2
70	90.0	R10_S2
74	101.9	R10_S2
78	121.6	R10_S2
84	146.5	R10_S2
99	185.1	R10_S2

2	1.5	R11_S1
6	49.5	R11_S1
9	117.3	R11_S1
15	114.4	R11_S1
22	145.8	R11_S1
34	174.1	R11_S1
48	171.3	R11_S1
51	5.9	R11_S2
56	24.1	R11_S2
62	63.2	R11_S2
70	113.2	R11_S2
74	134.4	R11_S2
78	134.6	R11_S2
84	133.8	R11_S2
99	132.2	R11_S2
4	36.1	R13_S1
7	41.1	R13_S1
13	212.8	R13_S1
20	389.4	R13_S1
34	407.2	R13_S1
46	418.2	R13_S1
54	108.8	R13_S2
60	181.8	R13_S2
68	219.9	R13_S2
72	245.8	R13_S2
76	297.8	R13_S2
82	346.4	R13_S2
97	420.0	R13_S2
103	433.1	R13_S2
111	49.9	R13_S3
116	186.3	R13_S3
120	205.2	R13_S3
124	257.6	R13_S3
130	302.0	R13_S3
4	174.9	R15_S1
7	216.0	R15_S1
13	246.1	R15_S1
20	256.8	R15_S1
34	250.4	R15_S1
46	245.3	R15_S1

54	1.0	R15_S2
60	5.0	R15_S2
68	10.0	R15_S2
72	15.4	R15_S2
76	69.5	R15_S2
82	117.1	R15_S2
97	184.0	R15_S2
4	102.7	R16_S1
7	125.7	R16_S1
13	291.5	R16_S1
20	444.3	R16_S1
34	477.9	R16_S1
4	99.2	R17_S1
7	114.9	R17_S1
13	265.0	R17_S1
20	398.0	R17_S1
34	410.4	R17_S1
46	411.6	R17_S1
54	50.0	R17_S2
60	155.6	R17_S2
68	262.7	R17_S2
72	307.7	R17_S2
76	372.6	R17_S2
82	429.8	R17_S2
97	536.1	R17_S2
103	566.6	R17_S2
111	30.5	R17_S3
116	164.7	R17_S3
120	254.8	R17_S3
124	340.1	R17_S3
130	401.3	R17_S3
4	56.4	R18_S1
7	72.0	R18_S1
13	204.0	R18_S1
20	386.5	R18_S1
34	430.9	R18_S1
46	435.6	R18_S1
54	57.4	R18_S2
60	180.5	R18_S2
68	239.8	R18_S2

72	289.2	R18_S2
76	354.7	R18_S2
82	397.6	R18_S2
97	445.6	R18_S2